A STUDY OF ISOTHERMAL VARIATION OF CONCENTRATION-DEPENDENT INTERDIFFUSION COEFFICIENT IN 100% Cu-100% Ni AND 50% Cu 50%Ni -100% Cu DIFFUSION COUPLES

BY

JULIANE GONCALVES LOPES

A Thesis submitted to the Faculty of Graduate Studies of the University of Manitoba in Partial Fulfillment of the Requirements for the Degree of

MASTER OF SCIENCE

Department of Mechanical Engineering,

University of Manitoba

Winnipeg

ABSTRACT

Concentration-dependent interdiffusion coefficients ($\widetilde{D}(C)$) are a fundamental parameter in the analysis of diffusion effects in materials. It is usually assumed in the literature that this parameter is mainly a function of concentration and temperature. However, recent studies have suggested that $\widetilde{D}(C)$ may also change with time isothermally due to the development of internal stresses and strains during the diffusion process.

The objective of this work is to verify if time affects the interdiffusion coefficient of a copper-nickel (Cu-Ni) system at a temperature range of 900°C-1000°C. A newly developed analytical method is used to address the shortcomings of conventional methods, such as the Boltzmann-Matano, Sauer-Freise and Hall techniques which neglect the presence of an initial solute distribution and therefore may produce unreliable results.

The results of this study show that $\widetilde{D}(C)$ of a Cu-Ni system indeed isothermally varies with time at all temperatures investigated as a result of diffusion-induced stress (DIS), in contrast to common assumptions in the literature. This finding draws attention to the need to take time into account as a fundamental factor in diffusion analysis, which would result in a more in-depth and accurate understanding of the interdiffusion phenomenon in materials.

ACKNOWLEDGMENTS

I would like to express my gratitude to my advisor, Dr. Olanrewaju Ojo. Throughout the duration of my master's program, Dr. Ojo provided invaluable support, guidance, and advice. His commitment and involvement in this project have greatly influenced my academic and personal growth, and I am grateful for his mentorship . I also extend my appreciation to Dr. Lina Zhang and Mike Boswick for their technical assistance in training and utilizing the laboratory equipment.

I want to acknowledge the support and encouragement of my loved ones. My husband, Patrick, for providing endless encouragement and understanding during my academic pursuit. To my parents, Vilmar and Francisca, and my sister, Aline, I am deeply thankful for their belief in me. Your support has been my source of motivation. To my in-laws, Angela and Jean-Marc, for providing support network for me here in Canada. And to my friends and coworkers for believing in my abilities and encouraging me to achieve my goals, I am grateful for each one of you.

LIST OF ABBREVIATIONS AND SYMBOLS

J: Flux

D: Diffusion coefficient

C: Concentration

t: Time

x: Distance

$\widetilde{D}$: Interdiffusion coefficient

DIS: Diffusion-induced stress

$\widetilde{D}$(C): Concentration-dependent interdiffusion coefficient

D_0: Pre-exponential factor

Q: Activation energy

R: Gas constant

T: Temperature

η: Boltzmann variable

C^*: Specific composition

x_M: Matano plane

y: Normalized concentration

B-M: Boltzmann-Matano

S-F: Sauer-Freise

A: Area

m: Mass of solute

V: Volume

D_{ave}: Average interdiffusion or average diffusivity

F: Force

Φ: Potential

T: Torque

k: Friction coefficient

D_p: Diameter of bolt

Common subscripts:

i: Initial

f: Final

L: Left

R: Right

TABLE OF CONTENTS

LIST OF TABLES

LIST OF FIGURES

1 INTRODUCTION

1.1 Background

Solid diffusion is the transport of matter from one point to another by the thermal motion of atoms within specific lattice sites. Diffusion is a fundamental process for understanding the kinetics of how temperature, time and concentration affect the microstructural changes that occur during material processing and heat treatment. Solid diffusion has a wide range of industrial applications, including semiconductor manufacturing, solution hardening, surface coating, and sintering processes. These applications rely on the controlled diffusion of atoms to achieve the desired physical and mechanical properties. Therefore, understanding solid diffusion enables advancements in the industry that rely on precise material engineering and processing techniques.

Diffusion can be described by using two equations that are known as Fick's First and Second Laws [1]. Fick's First Law states that the flux is proportionate to the concentration gradient, as follows:

$$J = -D \frac{\partial C}{\partial x} \tag{1.1}$$

Fick's Second Law predicts how diffusion causes concentration changes with time. The equation relates the rate of accumulation or depletion of the concentration with time to the second derivative of the concentration gradient as follows:

$$\frac{\partial C}{\partial t} = \frac{\partial}{\partial x}\left(D \frac{\partial C}{\partial x}\right) \tag{1.2}$$

Fick's equations introduce an important proportionality parameter known as the diffusion coefficient. The diffusion coefficient is a fundamental parameter that describes the ease and speed at which particles diffuse through a material. There are three types of diffusion coefficients – self-diffusion, intrinsic diffusion and interdiffusion coefficients [2]. Specifically, the interdiffusion

coefficient ($\widetilde{D}$) refers to the rate of diffusion of atoms between two different materials. In other words, this coefficient describes the intermixing of two elements of a diffusion couple.

In the literature, it is commonly accepted that the interdiffusion coefficient depends on both concentration and temperature [3], which implies that the coefficient remains constant over time under isothermal conditions. However, previous studies have presented data [4-11] to show that the interdiffusion coefficient varies as the annealing time changes. Despite these findings, most of these studies do not provide a clear explanation for the observed effect of time on the interdiffusion coefficient.

One potential explanation for the time effect on the interdiffusion coefficient is diffusion-induced stress (DIS). According to the literature [8, 12-21], DIS occurs during diffusion and is the result of differences in the intrinsic fluxes of a system, and the strain caused by lattice distortion during atom migration. The magnitude of DIS is closely related to the concentration gradient, as a larger concentration gradient, for example, means that diffusion takes place quickly, and potentially produces more stress.

Investigating the time effect on interdiffusion coefficient can provide a better understanding of the diffusion kinetics, which contributes to the development of more accurate models and simulations for predicting material behaviour. Furthermore, understanding the reason behind the time dependence of interdiffusion coefficient can provide information on the underlying factors that govern DIS and other microstructural changes that occur during material processing.

1.2 Thesis Hypotheses

Although it is widely accepted that the interdiffusion coefficient only depends on the concentration during isothermal processing, several works [4-11] have presented data that challenge this

assumption. The presence and development of DIS might be the cause for this phenomenon. The evolution of the concentration gradient over time influences the presence of stress in the diffusion system, which consequently affects the magnitude of the interdiffusion coefficient. Therefore, it may be possible that $\widetilde{D}(\mathrm{C})$ changes with time isothermally.

1.3 Thesis Objectives

The two main objectives of this work are:

1. To confirm the presence of a time effect on the interdiffusion coefficient in a copper-nickel (Cu-Ni) system. Then, if confirmed,
2. To determine the influence of concentration gradient changes on the interdiffusion coefficient, since the concentration gradient is closely related to DIS.

1.4 Scope

The scope of this thesis is to explore the time dependence of the interdiffusion coefficient in a Cu-Ni system at temperatures that range from 900°C to 1000°C. The influence of the concentration gradients and DIS associated with the time effect is also investigated.

1.5 Major Work Performed and Key Findings

In this work, diffusion annealing experiments with a Cu-Ni system for pre-determined times and temperatures are carried out. The resulting samples are analyzed by using an energy-dispersive x-ray (EDS) detector along with a scanning electron microscope (SEM) to obtain the concentration profiles for all of the conditions. The profiles are then smoothed by using the piecewise cubic hermite interpolating polynomial (PCHIP) function and the moving average method with developed MATLAB programs. After the data smoothing, additional programs are used to obtain the average concentration profiles and determine the interdiffusion coefficient. Error bars and *p*-

values, according to the *t-statistics* method, are obtained to plot the interdiffusion coefficient. Finally, the average diffusion coefficient (D_{ave}) is calculated for all of the conditions.

Through a careful examination of the obtained findings, this work reveals that the interdiffusion coefficient of a Cu-Ni system is indeed influenced by the diffusion time in the experiments performed. The results also show the major impact of the concentration gradient on the interdiffusion coefficient, thus indicating a connection to the DIS. Therefore, the time effect seen in the interdiffusion coefficient for this study can be the result of DIS.

1.6 Thesis Structure

This thesis consists of 5 chapters.

Chapter 1 provides the background information for this work, research hypothesis, objectives, major work performed and key findings, and the thesis structure.

Chapter 2 is the literature review. The first part of the chapter consists of a review of solid diffusion, diffusion mechanisms, and the equations that govern diffusion (Fick's laws). The second part of the chapter discusses the concept of diffusion coefficient, parameters that affect them and the different techniques to calculate $\widetilde{D}(C)$. The third part of the chapter reviews the effect of time as discussed in the literature and the concept of DIS.

Chapter 3 details the experimental work performed for this study. The first part of this chapter discusses the preparation of the starting materials and describes the annealing treatments carried out. The second part focuses on data treatment, including obtaining the average concentration profile for each sample, data smoothing and data reliability through the *t-statistic* method.

Chapter 4 provides the results of the interdiffusion coefficients for all conditions tested, as well as discussions on the time and concentration gradient effects as a result of DIS. The first part focuses

on the results of the Cu-Ni system at 900°C, 950°C and 1000°C for different periods of time to determine if the interdiffusion coefficients vary with time. The second part focuses on the influence of the initial uniform distribution of solute on the interdiffusion coefficient. Then, the third part details the interdiffusion coefficients of the systems with an initial non-uniform distribution of solute.

Chapter 5 provides the main conclusions for this study and a summary of the major findings.

Chapter 6 details the limitations of this work and recommendations for future research work.

2 LITERATURE REVIEW

2.1 Solid Diffusion

Solid diffusion is a fundamental process that occurs in various materials and important for determining processing parameters and material properties [20]. This process is defined as the spontaneous movement of atoms within a solid material, which is driven by thermal motion. This diffusion process leads to the rearrangement of atoms within the crystal lattice which leads to the reduction of concentration gradients and therefore the chemical potential energy.

2.1.1 Diffusion Mechanisms

Diffusion takes place in the crystal lattice through the presence of defects in solids. Point defects, which include for example, vacancies and interstitials, are responsible for the so-called volume or lattice diffusion [22]. Furthermore, diffusion can also take place through line defects, most commonly grain boundaries, through a high-diffusivity path [23]. The most common mechanisms of diffusion are summarized in the following sections, including vacancy, interstitial, interstitialcy, and grain boundary mechanisms of diffusion.

2.1.1.1 Vacancy Mechanism of Diffusion

Vacancies are unoccupied sites in a lattice. In vacancy diffusion, atoms migrate from one vacancy to a neighboring vacancy in order to move through the lattice. The rate of diffusion directly depends on the vacancy concentration, which has been observed to increase in higher temperatures [24]. This mechanism governs the self-diffusion of pure metals and diffusion of substitutional solutes in alloys [23]. Figure 2.1 shows the mechanism of vacancy diffusion, where a tracer atom is used to track the diffusion.

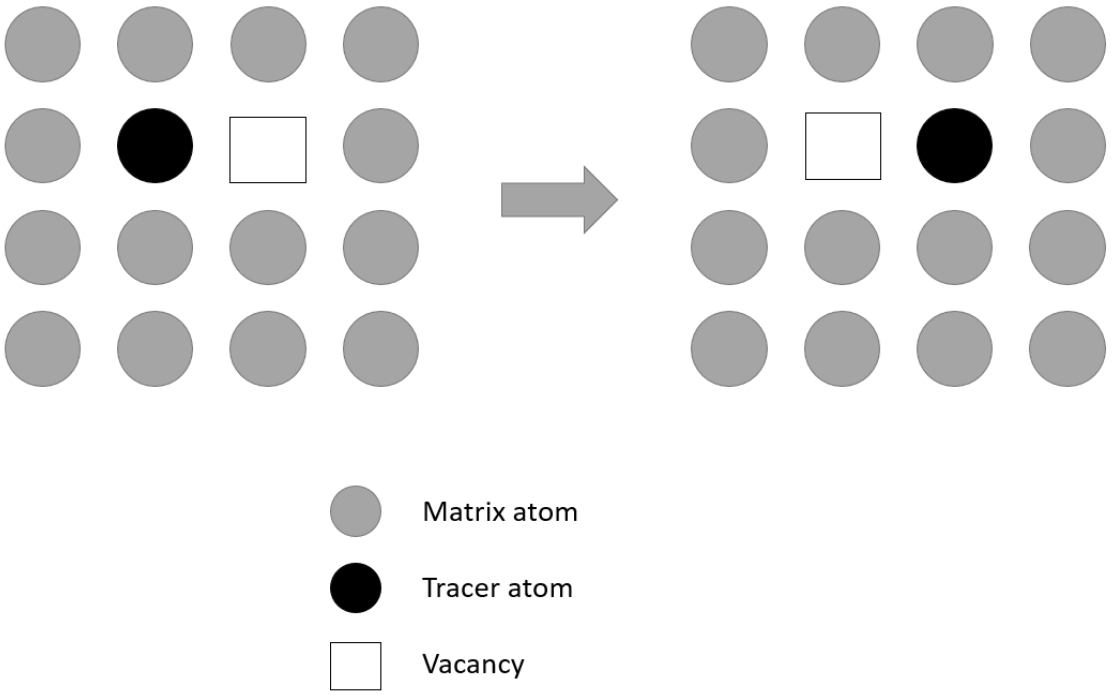

Figure 2.1. Vacancy mechanism of diffusion [1]

2.1.1.2 Interstitial Mechanism of Diffusion

Interstitial diffusion occurs when atoms jump into interstitial spaces in the host crystal lattice. The atoms are larger than the interstitial spaces, but their thermal energy allows them to occupy these sites temporarily. For this mechanism to take place, the solute atoms must be smaller than the host atoms [2]. Interstitial diffusion has a higher diffusion rate compared to vacancy diffusion due to the availability of neighboring interstitial sites. Figure 2.2 shows the interstitial mechanism of diffusion.

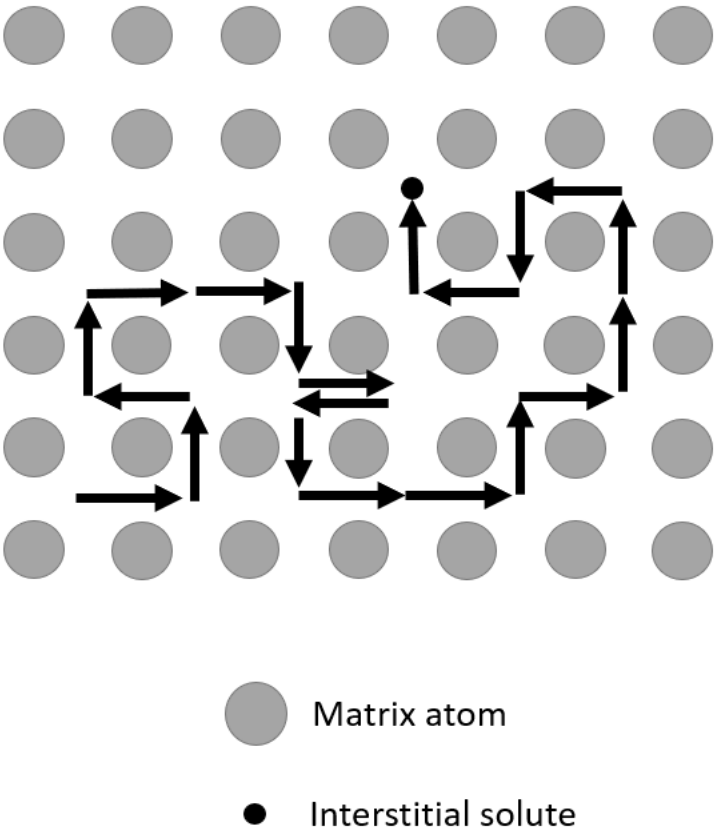

Figure 2.2. Interstitial mechanism of diffusion [1]

2.1.1.3 Interstitialcy Mechanism of Diffusion

In the interstitialcy mechanism of diffusion, a solute atom pushes a lattice atom into an interstitial site and in turn takes its place in the lattice. This mechanism is found with large solute atoms that would cause excessive distortion by only moving through the interstitial sites. This exchange happens in two stages, first the atom takes an interstitial position, and then subsequently, the atom switches position with a neighboring atom [2]. Figure 2.3 shows a schematic of this mechanism.

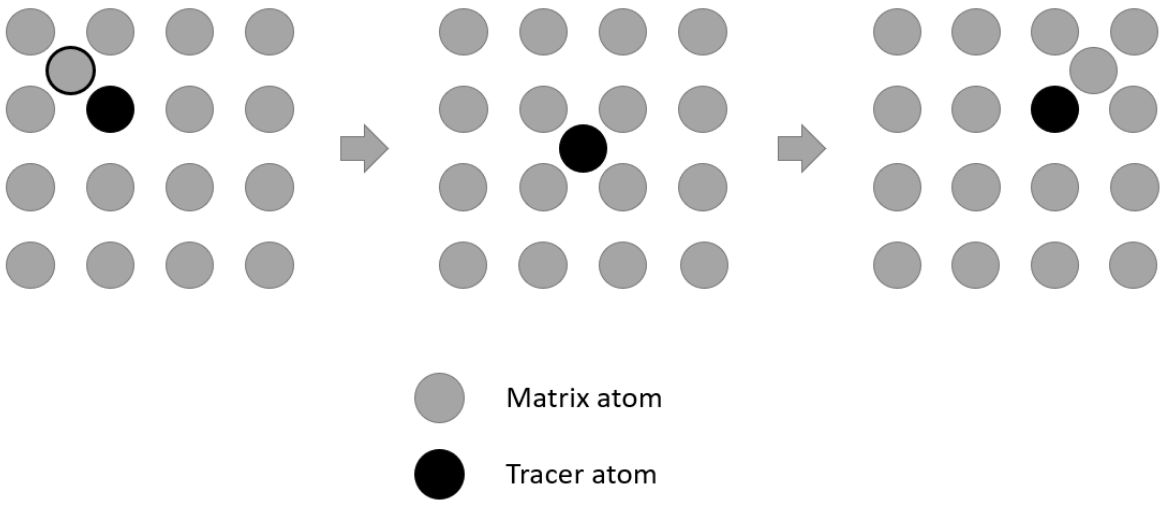

Figure 2.3. Interstitialcy mechanism of diffusion [2]

2.1.1.4 Grain Boundary Mechanism of Diffusion

The rate of diffusion can be increased when the diffusion process takes place through linear defects, mainly dislocations and grain boundaries. These defects provide a high-diffusivity path, also known as a short-circuit path for the atoms, where the jump frequency is about a million times more than that in the crystal lattice [23]. In grain boundary diffusion, the atoms move along the boundaries between neighboring grains through point defects. Vacancies within the grain boundaries are the most common point defects that mediate grain boundary diffusion [25]. Figure 2.4 shows the diffusion process along the grain boundaries as well as volume or lattice diffusion that is taking place simultaneously.

Several parameters influence the presence and magnitude of grain boundary diffusion; among the most relevant are grain size, grain orientation and temperature. In general, high angle boundaries are more efficient in providing diffusion paths than low angle boundaries due to the presence of lattice dislocations that tend to obstruct atom migration in the latter configuration [26]. Grain size

plays an important role in grain boundary diffusion, as a finer grain size means a larger density of grain boundaries, therefore providing more diffusion paths [25].

Furthermore, the volume diffusion is generally dominant for high temperatures, where the diffusion through the lattice is as quick or quicker than grain boundary diffusion [26, 27]. This is possible due to the increasing energy available for atoms to overcome energy barriers and move within the bulk, as well as the increased vacancy concentration.

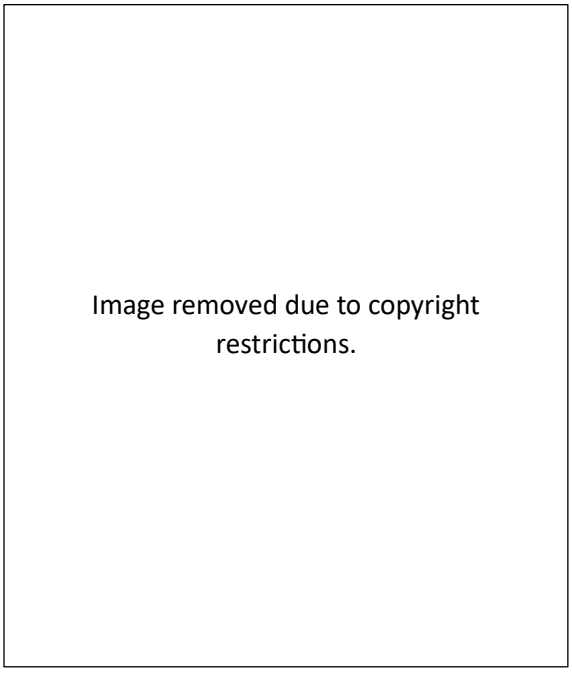

Figure 2.4. Grain boundary and lattice diffusion [28]

2.2 Diffusion Equations

In the mid-19th century, Adolf Fick, German physiologist, developed two fundamental equations to mathematically describe the behaviour and principles of diffusion. Fick's laws relate the diffusion flux to the concentration gradient and their formulation will be explained in the following sections.

2.2.1 Fick's First Law

In an inhomogeneous material, the atom flow tends to move in a manner that reduces the concentration gradients. Once the material is homogeneous, the net flux will stop. Fick's First Law [22] establishes that the flux is proportional to the concentration gradient, which is described by using:

$$J = -D \frac{\partial C}{\partial x} \qquad 2.1$$

where J is the diffusion flux and C is the concentration. The proportionality parameter D is the diffusion coefficient, given in m^2/s. The negative sign of the equation indicates the direction of the flux, from regions of higher concentration to regions of lower concentration, in order to reach equilibrium.

2.2.2 Fick's Second Law

Fick's First Law is only applicable to steady-state systems, where the concentration does not change with time. If the steady-state assumption does not hold, Fick's Second Law is applicable. This law relates the change in concentration with time to the second derivative of the change in concentration with space, and described by using:

$$\frac{\partial C}{\partial t} = \frac{\partial}{\partial x}\left(D \frac{\partial C}{\partial x}\right) \qquad 2.2$$

2.3 Diffusion Coefficient

The diffusion coefficient is the proportionality parameter given in Fick's laws that relates diffusion flux to the concentration gradient. This coefficient describes the rate at which a material diffuses through a medium. There are different types of diffusion coefficients, including impurity, intrinsic

and tracer diffusion coefficients; however, this work will only discuss the interdiffusion coefficient. The interdiffusion coefficient and its influential parameters are discussed in the following sections.

2.3.1 Interdiffusion Coefficient

The interdiffusion coefficient describes how the components of system or an alloy diffuse into each other. In other words, this coefficient measures the rate of mixing between two elements of a diffusion couple [29]. It is generally denoted as $\widetilde{D}$ and measured in square meters per second (m^2/s).

The interdiffusion coefficient is a single parameter that quantifies the diffusion of binary systems driven by chemical inhomogeneity. This coefficient provides insight into how a material will interact and change over time, which facilitates a better understanding and control of diffusion processes.

2.3.1.1 Composition Dependence of Interdiffusion Coefficient

The chemical potential, which arises from concentration gradients in a binary system, drives diffusion. As diffusion progresses and these gradients shift, it is expected that the interdiffusion coefficient also varies. Consequently, one of the most fundamental factors that affects the interdiffusion coefficient is the solute concentration. The concentration-dependence can be weak, so that the interdiffusion coefficient remains almost constant throughout the concentration range [30] or lead to $\widetilde{D}(C)$ varying up to two orders of magnitude as the concentration changes [31, 32]. Several factors can contribute to the concentration-dependence of the interdiffusion coefficient; among them are:

1. Phase transformations: as the microstructure evolves, the interdiffusion coefficient can change due to diffusion mechanisms or diffusion path changes with a new phase [32, 33].

2. Diffusion mechanisms: the interdiffusion coefficient is also subject to change with the presence of lattice defects such as vacancies, interstitials, or grain boundaries [27, 34]. As discussed in Section 2.1, different diffusion mechanisms can lead to a significant difference in the diffusion rate.
3. Atomic size: when there is a large atomic size mismatch of the different phases, the interdiffusion coefficient can decrease as the concentration approaches the critical point [33, 35].
4. Melting temperature: Shewmon [23] discussed how in binary systems, the interdiffusion coefficient increases as the content of the species with a lower melting point increases because of their higher thermal vibration energy. Several other works [4, 34-36] have also experimentally observed this trend.

2.3.1.2 Temperature Dependence of Interdiffusion Coefficient

The interdiffusion coefficient is also exponentially dependent on the annealing temperature. As the temperature increases, there is more thermal energy available for atom movement and therefore, the diffusion flux increases as well. There is general consensus in the literature that the interdiffusion coefficient is governed by the Arrhenius equation, which is:

$$\widetilde{D} = D_0 \exp\left(-\frac{Q}{RT}\right) \qquad 2.3$$

where D_0 is the pre-exponential factor, Q is the activation energy, R is the gas constant and T is the temperature.

2.4 Conventional Methods to Calculate Interdiffusion Coefficient

For single-phase binary systems, the interdiffusion coefficient can be obtained by using conventional analytical techniques that consider the experimental concentration profile of the system [37]. The most common methods are the Boltzmann-Matano (B-M) and Sauer-Freise (S-F) methods, which will be detailed in the upcoming sections.

2.4.1 Boltzmann-Matano Method

The B-M method was developed by Matano [38] who extended Boltzmann's transformation [39] and introduced the Matano plane. Boltzmann's transformation $\eta = x/\sqrt{t}$ is applied to Fick's Second Law to give:

$$-2\eta\frac{dC}{d\eta} = \frac{d}{d\eta}\left(D\frac{dC}{d\eta}\right) \qquad 2.4$$

Considering two semi-infinite bars as the diffusion couple, Matano [38] proposed the following initial boundary conditions:

$C = C_L$ for $(x < 0, t = 0)$

$C = C_R$ for $(x > 0, t = 0)$

Integrating Equation 2.4 with $\int_{C_L}^{C^*} dC$, results in:

$$-2\int_{C_L}^{C^*}\eta dC = \widetilde{D}\left(\frac{dC}{d\eta}\right)_{C^*} - \widetilde{D}\left(\frac{dC}{d\eta}\right)_{C_L} \qquad 2.5$$

If $(dC/dx)_{C_L} = 0$, Equation 2.5 can be rewritten as:

$$\widetilde{D}(C^*) = -2\frac{\int_{C_L}^{C^*}\eta dC}{(dC/d\eta)_{C=C^*}} \quad 2.6$$

Substituting the Boltzmann variable (η) back in leads to the final equation to calculate the interdiffusion coefficient:

$$\widetilde{D}(C^*) = -\frac{1}{2t}\frac{\int_{C_L}^{C^*}(x - x_M)dC}{(dC/dx)_{C^*}} \quad 2.7$$

where x_M is the Matano plane, which is:

$$\int_{C_L}^{C_R} x dC = 0$$

The law of conservation of mass is satisfied on the Matano plane. In other words, the Matano plane represents the point where the reduction of matter on one side of the interface is equal to the accumulation of matter on the other side [40]. The B-M method is the most commonly used method to calculate the interdiffusion coefficient for binary couples due to its simplicity and practicality. On the other hand, the accuracy of this method relies on finding the location of the Matano plane and evaluating the slope [41]. Furthermore, the B-M method does not predict the interdiffusion coefficient accurately for the extreme ends of the concentration profile [38].

2.4.2 Sauer-Freise Method

The S-F method was developed to address the problem of having to accurately calculate the Matano plane position [42]. The method calculates the interdiffusion coefficient as a function of concentration by introducing a normalized concentration variable, given as:

$$y = \frac{C - C_R}{C_L - C_R}$$

where the subscripts R and L represent the left and right sides of the concentration profile. The S-F solution to find the interdiffusion coefficient is:

$$\widetilde{D}(C^*) = -\frac{1}{2t}\left(\frac{dx}{dC}\right)_{C^*}\left[(1-y)\int_{x^*}^{+\infty}(C^* - C_R)dx + Y\int_{-\infty}^{x^*}(C_L - C^*)dx\right] \qquad 2.8$$

2.4.3 Step-Function Assumption

The conventional methods to calculate the interdiffusion coefficient mentioned in the previous section are based on the assumption that the initial state of the diffusion couple has no initial solute. This condition is commonly known as the step-function assumption. The step-function assumption limits the use of the conventional methods for processes that involve multiple diffusion steps, such as diffusion brazing, coating, and electroplating. Thus, the presence of an initial solute distribution leads to errors in calculating the interdiffusion coefficient with commonly used techniques, such as the B-M or S-F methods. This error is more pronounced for short annealing times because the error decreases with increasing diffusion time [43, 44].

2.5 Two-Profile Method to Calculate Interdiffusion Coefficient

In order to calculate the interdiffusion coefficient for short-time samples with an initial solute distribution, and the interdiffusion coefficient between time intervals, a two-profile approach developed by Olaye and Ojo [45] to modify the conventional methods was used. The following sections will detail the developed equations.

2.5.1 Two-Profile B-M Method

Starting with Fick's First Law (*Equation 2.1*), a section of the concentration profile in the unidirectional system is taken, where the area is given as:

$$dA = (x_f - x_i)dC \tag{2.9}$$

where dA is the area, dC is the change in concentration, and x_f and x_i are the distance for the final and initial profiles respectively. Relating the concentration to the amount of solute (m) and volume, dC can be rewritten as:

$$dC = \frac{dm}{V} = \frac{dm}{A(x_f - x_i)} \tag{2.10}$$

Substituting *Equation 2.10* into *Equation 2.9* gives:

$$dA = (x_f - x_i)dC = \frac{(x_f - x_i)dm}{A(x_f - x_i)} = \frac{dm}{A} \tag{2.11}$$

Integrating *Equation 2.11* and dividing by time, results in:

$$\frac{A}{\Delta t} = \frac{1}{\Delta t}\int_{C_R}^{C^*}(x_f - x_i)dC = \frac{1}{\Delta t}\int_{C_R}^{C^*}\frac{dm}{A} = \frac{m}{A\Delta t} \tag{2.12}$$

The flux is given as:

$$J = \frac{m}{A\Delta t} \tag{2.13}$$

Equations 2.12 and *2.13* can be combined to give:

$$J = \frac{m}{A\Delta t} = \frac{1}{\Delta t}\int_{C_R}^{C^*}(x_f - x_i)dC \qquad 2.14$$

Substituting *Equation 2.14* into *Equation 2.1* and solving for the diffusion coefficient leads to:

$$D = \frac{\overline{dx}}{dC}\frac{\int_{C_R}^{C}(x_f - x_i)dC}{\Delta t} \qquad 2.15$$

where $\frac{dx}{dC}$ is the inverse concentration gradient [46]. Equating *Equation 2.7*, which is the B-M solution for Fick's Second Law to *Equation 2.15* gives:

$$\frac{\overline{dx}}{dC} = \frac{1}{2t}\frac{dx}{dC} \qquad 2.16$$

For a two-profile system, the inverse concentration gradient can then be described as:

$$\frac{\overline{dx}}{dC} = \frac{1}{2}\left(\frac{dx}{dC_i} + \frac{dx}{dC_f}\right) \qquad 2.17$$

Including the inverse concentration gradient in *Equation 2.7*, the B-M formula for a two-profile approach is:

$$D = -\frac{1}{2}\left(\frac{dx}{dC_i} + \frac{dx}{dC_f}\right)\frac{\int_{C_R}^{C}(x_f - x_i)dC}{\Delta t} \qquad 2.18$$

This equation is only valid when the Matano plane is the same for the initial and final profiles.

2.5.2 Two-Profile Sauer-Freise Method

Applying the same methodology to the S-F method, the equation to find the interdiffusion coefficient is:

$$D = -\frac{1}{2}\left(\frac{dr}{dy_i}+\frac{dr}{dy_f}\right)\left[\frac{\left((1-y^*)\int_{-\infty}^{r^*} y\,dr_f + y^*\int_{r^*}^{+\infty}(1-y)\,dr_f\right)-\left((1-y^*)\int_{-\infty}^{r^*} y\,dr_i + y^*\int_{r^*}^{+\infty}(1-y)\,dr_i\right)}{\Delta t}\right] \quad 2.19$$

Since there is no need to find the location of the Matano plane, this method is used in this study.

2.6 Average Interdiffusion Coefficient

The average interdiffusion coefficient (D_{ave}) is the average single value of the interdiffusion coefficient for a certain concentration range. Since the interdiffusion coefficient changes with concentration, D_{ave} represents the diffusivity of the system for specific conditions, such as the temperature. D_{ave} is calculated as:

$$D_{ave} = \frac{\int_{C_L}^{C_R} D dC}{C_R - C_L} \quad 2.20$$

2.7 Time Variation of Interdiffusion Coefficient

It is a common assumption in literature that interdiffusion coefficient diffusion is independent of time [40], therefore, the majority of the available studies present data for only one annealing time for a particular temperature. Despite this assumption, the available data [4-11] show that the interdiffusion coefficient changes as the annealing time changes.

Campbell et al. [4] carried out diffusion experiments from 115°C to 173°C for a system that consists of lead (Pb) and Pb-50 wt. % indium (In) and used the B-M method to obtain the interdiffusion coefficient. The authors provided data for the average interdiffusion coefficient across various annealing times. At 115°C, the annealing times were 256.5 and 1230.5 hours for Pb and Pb-50 wt. In %, respectively; at 129°C, 110 and 581.8 hours; at 149°C, 40 and 264.7 hours; and at 173°C, 18 and 118 hours. Among these experiments, the most significant variation of the interdiffusion coefficient was observed at 149°C. According to the findings, $\widetilde{D}(C)$ increases from

1.9×10^{-10} cm^2/s to 2.8×10^{-10} cm^2/s as the annealing time is increased from 40 hours to 264.7 hours, which is an increase of 47.4%.

Kucera et al. [5] calculated the interdiffusion coefficient of a cobalt (Co)-Ni system at a high temperature range (950-1150°C) by using the B-M method. At 1150°C, Kucera et al. [5] report a maximum increase of 114.7% for the interdiffusion coefficient as the annealing time was increased from 9 to 16 hours. As the annealing time was further increased to 49 hours, the interdiffusion coefficient showed a subsequent decrease of 24.8%. In an earlier study by Haebicek et al. [6] who used the same system and methodology, the interdiffusion coefficient is increased by 63.5% as the annealing time is increased from 4 to 36 hours.

Kirkendall et al. [7] examined a Cu-zinc (Zn) system by electroplating pure Cu onto brass strips with different Zn compositions. The authors used a graphical method to calculate the average constant diffusion coefficient between two concentration profiles. For Cu and Cu- 57.52 at. % Zn, the D_{ave} increases up to 70.8% for the time intervals of 1-4 hours and 4-10 hours. It should be noted that the method used in Kirkendall et al. [7] does not account for the concentration dependence of the interdiffusion coefficient; therefore, their method would not provide accurate results for this study.

The authors in [9], [10] and [11] provided indirect evidence of the effect of time by presenting concentration profiles for different annealing times or interdiffusion coefficient versus concentration plots. Olaye and Ojo [8] calculated the interdiffusion coefficient between time intervals for an Ni-rhenium (Re) system at 1050°C which was described in [9] by using a numerical analysis approach. Figure 2.5 shows the clear difference in magnitude of the interdiffusion coefficient. In [10], the change in chemical diffusivity in α brass throughout the Zn composition

range is reported for 223 and 501 hours at an annealing temperature of 700°C. Mehl and Rhines [11] determined the rate of diffusion for seven systems: Cu-Zn, Cu-aluminium (Al), Cu-beryllium (Be), Cu-cadmium (Cd), Cu-silicone (Si) and Cu-tin (Sn). The annealing temperatures ranged from 500 to 900°C, while the diffusion times spanned from 1.31 to 86 days. For each system and at least one temperature, different plotted curves of the interdiffusion coefficient across the solute concentration range were observed.

Olaye and Ojo [8] presented a novel numerical analysis approach to calculate $\widetilde{D}$(C). They used the silver (Ag)-Cu solid-liquid and Cu-Ni solid-solid systems, as well as data from other studies to calculate interdiffusion coefficients as a function of concentration and time. For the Ag-Cu system, the average diffusivity decreases by 57% as the diffusion intervals shift from 1-5 hours to 5-25 hours. Similarly, in the Cu-Ni system, the average diffusivity decreases by 65% as the time intervals increase from 1-10 hours to 25-72 hours.

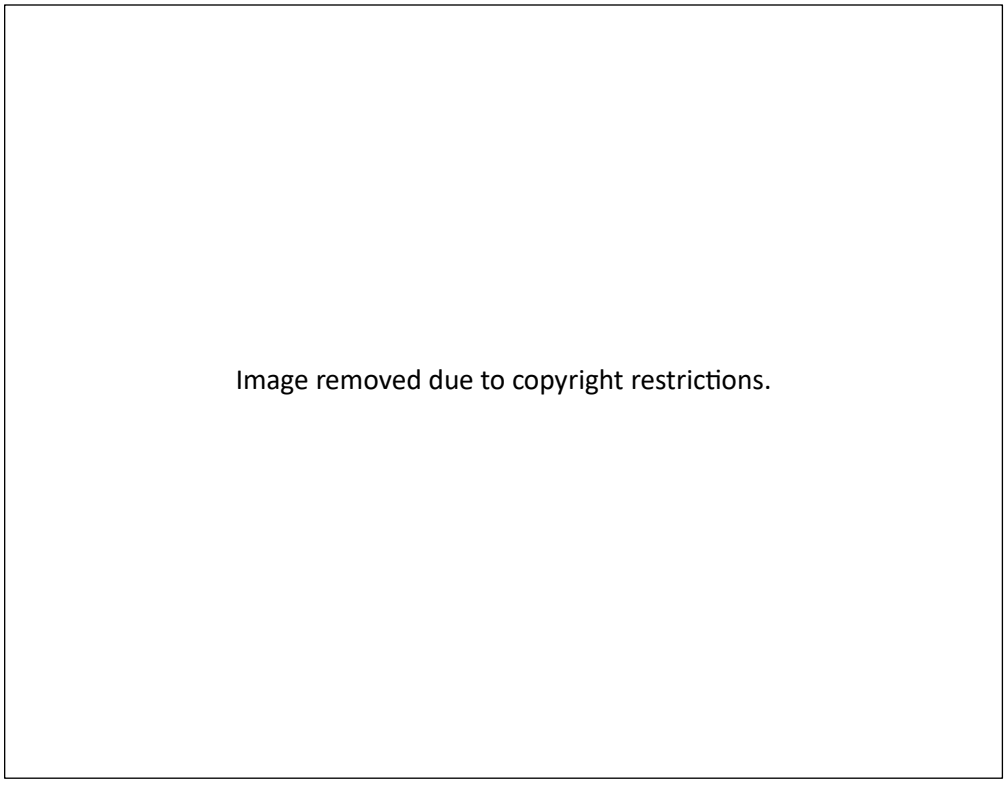

Figure 2.5. Variation of interdiffusion coefficient with concentration for Ni-Re system at 1050°C [8]

The change in the $\widetilde{D}$(C) with time could be attributed to grain boundary diffusion, or the presence of residual stresses. In this study, the experiments are carefully executed to eliminate the possibility of grain boundary diffusion or residual stress influencing the interdiffusion coefficient. Aside from the previously listed factors, another phenomenon that could cause the interdiffusion coefficient to change with time is the presence and evolution of DIS.

2.7.1 Diffusion-Induced Stress

DIS refers to the internal stresses that are generated due to the atom movement within a material. During diffusion, atom movement can create imbalances in the lattice structure of the material thus causing stresses that can induce mechanical strain. In the literature, this phenomenon is mostly

studied for thin sheets [15, 16, 46, 47], in which the effects can be clearly observed in the form of bending.

The emergence of internal stresses leads to changes in the energy that governs the movement of atoms, also known as the thermodynamic potential for diffusion. Figure 2.6 shows the origin and effects of DIS in the diffusion process.

The cause of DIS can be attributed to the volume changes associated with atomic diffusion, caused by the difference in atomic size or intrinsic diffusion coefficients, or the development of intermetallic phases [19]. Since the Cu-Ni system is completely soluble, and the atomic sizes of Cu and Ni are similar [48], the generation of DIS in the system is attributed to the difference in intrinsic diffusion coefficients. Previous studies [47, 49, 50] have shown that Cu has a higher diffusivity than Ni in a Cu-Ni system, which further validates that the DIS generated in this system stems from the volume changes generated from one side of the diffusion couple that is expanding while the other side is contracting. In general, the highest stresses develop at the beginning of the diffusion process. As the process evolves, the stress decreases as a result of the decrease in concentration gradient [51].

As the magnitude of the internal stresses increases, the material also undergoes relaxation to reach a lower-state energy and reduce stress levels. This relaxation phenomenon happens through plastic deformation and takes longer than stress to be generated during diffusion [14]. This time discrepancy between stress buildup and relaxation renders the relaxation of the internal stresses step a potentially limiting factor of interdiffusion [21].

In the absence of other fields or interfaces, the only driving force for diffusion is the chemical potential. The chemical potential gradient is conveniently expressed in terms of a concentration

gradient. Essentially, this means that atoms move from areas of higher concentration to those of lower concentration until the chemical potential energy is the same across the material. As described in Fick's First Law, the diffusional flux and change in concentration gradient can be related by using a diffusion coefficient parameter.

The diffusion flux, and therefore the diffusion coefficient, can also change with the presence of additional driving forces, e.g., electrical, thermal, magnetic or stress fields. For this series of experiments of binary couples without external forces, only the chemical potential and stress potential (generated by diffusion) are present. Therefore, the driving forces of diffusion can be expressed as:

$$\overrightarrow{F_1} = -\nabla\Phi_1 = -\nabla\mu_{chemical} \,\&\, \nabla\mu_{stress} \qquad 2.21$$

where Φ_1 is the thermodynamic potential for diffusion. *Equation 2.21* is merely representative, the chemical and stress potential can be further discretized, but this work will not provide the complex solutions for DIS. As a result, DIS will not be directly calculated here.

Additionally, since this study uses bulk planar diffusion couples, no bending can be seen as a result of DIS. Therefore, an indirect investigation of the presence of DIS is proposed through the concentration gradient. The concentration gradient drives the diffusion process, while the resulting atomic flux creates non-uniformities in the material, which lead to the generation of internal stresses. The assumption is that the interdiffusion coefficient is influenced by the concentration gradient changes because of DIS. As the concentration gradient changes with diffusion time, the presence of DIS is the most likely reason for the changes in the interdiffusion coefficient with time during isothermal diffusion.

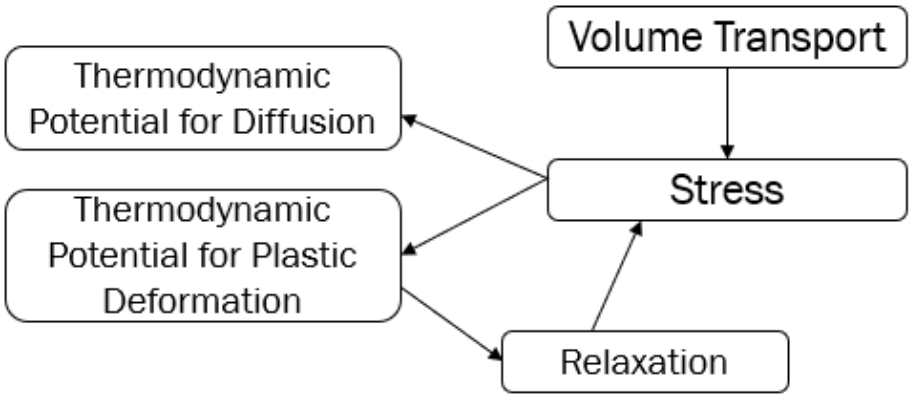

Figure 2.6. Schematic of DIS in a binary diffusion couple [19]

3 METHODOLOGY

3.1 Starting Materials

The materials chosen for this study are pure Cu and Ni, and Cu-50 at. % Ni, an alloy that contains an atomic composition of 50 percent of Ni and 50 percent of Cu. The materials were obtained from ACI Alloys Inc. (USA). After cold rolling, the alloy samples were encapsulated in quartz capsules filled with argon gas and subsequently heat treated at 1030°C for 75 hours. The intent of this heat treatment is to promote further composition homogenization of the alloy. Table 3.1 shows the constituents of the chosen binary diffusion couples and their composition.

Table 3.1 Binary diffusion couples

Diffusion Couple	Material A	Material B
Pure Element Couple	Pure Cu (100% at. Cu)	Pure Ni (100% at. Ni)
Alloy Couple	$Cu_{50}Ni_{50}$ (50% at. Ni)	Pure Cu (100% at. Cu)

3.2 Sample Preparation

The metallographic preparation of the samples and fabrication of the diffusion couples in this study are described in the following sections.

3.2.1 Heat Treatment of Starting Materials

All of the materials used in this study are first cold rolled to about 1.5 mm in thickness. Cold rolling is known [52-54] to increase the density of dislocations and introduce considerable stress into materials due to plastic deformation. Dislocations, like grain boundaries, are linear defects that can increase the diffusivity through the so-called short-circuit paths. Therefore, in order to provide stress relief and induce recrystallization, the samples were encapsulated in quartz capsules filled with argon gas and heat treated at 1030°C for 4 hours.

The selected temperature exceeded the recrystallization and stress relief temperature thresholds for Cu and Ni [55-57]. As a result, the samples were subjected to an isothermal heat treatment for 60 minutes to provide stress relief and induce recrystallization [58].

Moreover, the annealing temperature and duration are well-suited for promoting the growth of large grains in order to minimize the impact of grain boundary diffusion. Olaye and Ojo [8] showed that grain growth does not cause significant changes between a 1-hour heat treatment and one that extends up to 72 hours. For that reason, 4 hours is a sufficient timeframe for heat treatment at 1030°C to achieve the desired outcomes of stress relief, recrystallization, and grain growth.

3.3 Diffusion Coupling Technique

After the heat treatment took place as described in Section 3.2, the samples were metallographically prepared in which their surface was grinded with 240, 600 and 1200 grit sandpaper followed by polishing with 3 μm and 1 μm diamond suspension solutions, respectively. The intent of the metallographic preparation is to provide a flat and smooth surface for bonding, as well as removing the passivating film on the materials. The samples were then subjected to ultrasonic cleaning to remove any contamination that might have been present on the surface. Prior to bonding, the outer surface of the samples was coated with *NICROBRAZ Green Stop-off,* a product used to create a barrier or protective coating and impede the flow of brazing filler material. In this experiment, the *NICROBRAZ Green Stop-off Type I Pen* was used to impede the diffusion between the samples and the assembly jig for the diffusion couple.

The diffusion coupling technique consists of providing enough contact between two or more materials in which diffusion will occur between them. In most cases, force needs to be applied to the assembly jig to promote further contact [59]. The steel jig used in this study consists of four

bolts tightened to 15-20 ft·lbs, as shown in Figure 3.1. In order to convert the torque into axial load, the following equation is used:

$$T = k \cdot F \cdot D_p \qquad 3.1$$

where T is torque in lbf·in, k is the coefficient of friction which in this study is 0.2 and applicable for all types of bolts, F is the axial load in lbf, and D_p is the bolt diameter, which is 0.375 inches. The axial load for each bolt was calculated to be 2.4-3.2 kips.

The next step was to perform the heat treatment to promote diffusion bonding. The entire ensemble was annealed in a high vacuum furnace (GCA Corporation) at 600°C for 1 hour.

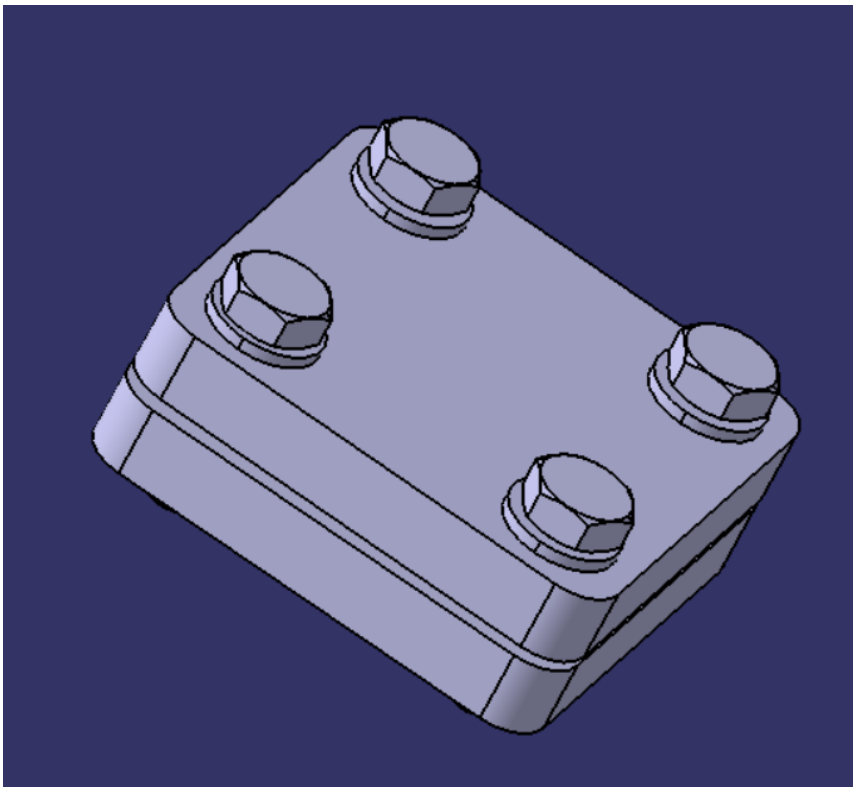

Figure 3.1. Schematic of steel assembly jig

3.4 Electroplating

The next stage that followed the diffusion bonding was to electroplate the diffusion couples with Ni to further protect the samples from oxidation.

The couples were first grinded to remove the stop-off pen coating and create a better surface for electrodeposition. Chemical cleaning was then performed in four stages:

1. Immersing the samples in a boiling mixture of sodium hydroxide (NaOH), sodium carbonate (Na_2Co_3) and disodium hydrogen phosphate (Na_2HPO_4) for 20 minutes.
2. Using an immersion bath with a 30% solution of hydrochloric acid (HCl) for 5 minutes at room temperature.
3. Placing the couples in a boiling 10% solution of sulfuric acid (H_2SO_4) for 3 to 5 minutes.
4. Using a 5% solution of sulfuric acid for 1 minute at room temperature.

The cleaning is essential to ensure that no contaminants are present, and that the deposited material will adhere to the surface. Following cleaning, the couples were placed in an electrolytic bath which consisted of a solution of nickel sulfate hexahydrate ($NiSO_4 \cdot 6H_2O$), nickel chloride hexahydrate ($NiCl_2 \cdot 6H_2O$) and boric acid (H_2BO_3). Figure 3.2 shows the schematic of the electroplating setup, where the anode is a pure Ni rod, the reference electrode is a saturated calomel electrode (SCE) and the cathode is the diffusion couple onto which the electrodeposition would take place. The current chosen based on the surface area is 10 mA/cm^2, the time chosen for the procedure is 8000 seconds, and the electroplating apparatus used is a potentiostat galvanostat (*VersaSTAT3*).

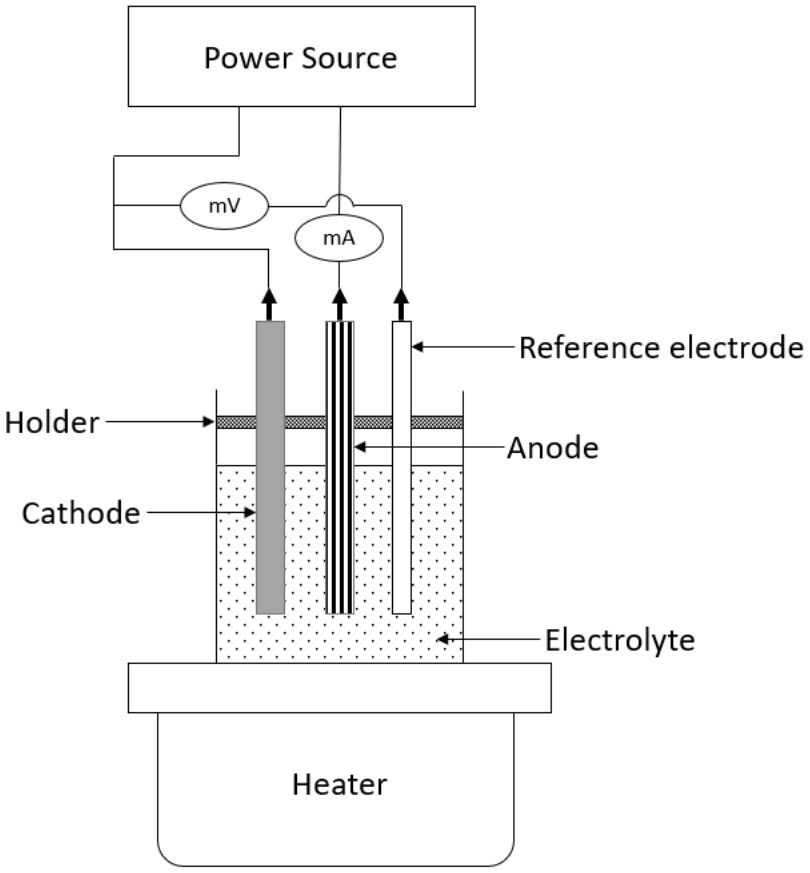

Figure 3.2. Electroplating apparatus [60]

3.5 Isothermal Annealing

After the diffusion couples were electroplated, the specimens were placed into quartz capsules filled with argon gas. The diffusion heat treatments were performed in two different stages; that is, single- and multi-stages for the Cu-Ni system. The multi-stage experiments included an initial annealing stage followed by the same heat treatment that was used in the single-stage experiments. The annealing times and temperatures for the single- and multi-stage experiments are given in Tables 3.2 and 3.3, respectively.

Table 3.2 Diffusion annealing parameters for single-stage experiments

Annealing Temperature	Annealing Times	Diffusion Couples
900°C	5 hours, 25 hours, 75 hours, and 150 hours	Cu-Ni, Cu-50 at. % Ni
950°C	5 hours, 25 hours, 75 hours, and 150 hours	Cu-Ni, Cu-50 at. % Ni
1000°C	5 hours, 25 hours, 75 hours, and 150 hours	Cu-Ni, Cu-50 at. % Ni

Table 3.3. Diffusion annealing parameters for multi-stage experiments

Initial Stage	Annealing Temperature	Annealing Times	Diffusion Couple
900°C for 5 hours (Type I)	950°C	5 hours, 25 hours, 75 hours, and 150 hours	Cu-Ni
1000°C for 5 hours (Type II)	950°C	5 hours, 25 hours, 75 hours, and 150 hours	Cu-Ni

Three annealing temperatures and four different annealing times were used in the single-stage experiments, which required a total of 12 samples for each binary system. Three annealing temperatures and four different annealing times were also used in the multi-stage experiment, but two initial annealing stages (Types I and II) were included, so a total of 24 samples were required for each binary system.

3.6 Concentration Profile Measurement

After the diffusion experiments were conducted, the couples were sectioned and mounted in Bakelite for the subsequent metallographic preparation process. The samples were grinded by using 240, 600, and 1200 grit sandpaper followed by polishing with 3 μm and 1 μm diamond suspension solutions, respectively. The composition points across the diffusion zone were measured by using an EDS detector along with an SEM (*JEOL JSM-5900LV)*.

The composition points were measured in steps that varied from 2 to 6 μm, depending on the penetration depth of the sample. At least six concentration profile readings were taken for each sample.

3.7 Data Smoothing

The concentration profile data contained noise which was removed in two stages: using the simple moving average method, followed by applying the PCHIP function, which is a numerical method to interpolate data. The simple moving average method is a statistical technique used to calculate the average value of a set of numbers to provide the central tendency of a data set. Symmetric moving average is used in this work, for which data points both before and after the current point are considered in the window. The simple moving average formula is:

$$Moving\ Average = \frac{(X_k - m + X_k - m + 1 + \cdots + X_k - 1 + X_k + X_k + 1 + \cdots + X_k + m)}{(2m + 1)} \quad 3.2$$

where $X_k - m, X_k - m + 1, \ldots, X_k - 1, X_k, X_k + 1, \ldots, X_k + m$ are the data points and m is the number of data points. Following the symmetric moving average filter, the concentration profile is smoothed by using the PCHIP function, which provides a smooth interpolation by plotting a polynomial curve based on the slopes of the data points [61]. The accuracy of the calculated interdiffusion

coefficient greatly depends on the degree of smoothness of the concentration profiles. An overly smoothed profile will result in larger interdiffusion coefficients. Therefore, the smoothed concentration profile was compared to the raw data for each sample to ensure that the profile shape remained relatively unchanged.

3.8 Average Concentration Profile

The average concentration profile for every sample was obtained by using concentration profiles acquired from six different locations. The individual profiles were lightly smoothed with the spline function in MATLAB. This initial smoothing process was to eliminate exceptionally noisy data. The smoothed individual profiles were then compared to the raw data to confirm that the new profiles are still representative and not excessively smoothed.

Next, the six concentration profiles were aligned with their respective Matano interfaces and the average distance for each concentration point was calculated. The resulting average concentration profiles were then subjected to another round of smoothing with the method described in Section 3.7.

3.9 Error Bars and Determining Error Margin

For the interdiffusion coefficient and concentration plots, error bars are used to represent the uncertainty of a data set. The bars extend from each data point to indicate the range of possible values that the data point can represent. In this study, the error bars for each condition are calculated based on the standard deviation of a data point, which represents the data dispersion [62].

The D_{ave} values were calculated for the six different profiles for each time and temperature condition. The relative error percentage was obtained by comparing these results to the D_{ave} values obtained from the average concentration profile. The maximum variation was observed to be 14%,

which is in agreement with the error observed for the interdiffusion coefficient in [8] for the Cu-Ni system.

3.10 T-Statistics

The statistical reliability of the interdiffusion coefficients calculated in this work is determined by using *t-statistics*. *T-statistics* are used to test the observed difference between a sample mean and a population mean, relative to the variability within the sample, and helps to determine whether the observed difference is statistically significant or simply due to random sampling variability. This inferential statistic quantifies the extent to which the sample mean deviates from the hypothesized population mean.

In this study, the two-sample method is used in which two independent populations are compared. For unequal variances, the formula is:

$$T = \frac{(\bar{X}_1 - \bar{X}_2)}{\sqrt{\frac{S_1^2}{n_1} + \frac{S_2^2}{n_2}}} \qquad 3.3$$

where T is the calculated t-statistic, $\bar{X}$ is the sample mean, n is the sample size, and S is the sample standard variation. For unequal variance, the *t-statistic* is considered robust for equal and large enough sample sizes [63]. In this work, the sample size is 36, which is considered large for minimal error. The *p-value* is the parameter that quantifies the statistical difference between the two sets of data. For this work, the commonly used threshold value of 0.05 (5%) is used. In other words, if $P < 0.05$, the interdiffusion coefficient values are considered statistically different, and when $P > 0.1$, the values are considered statistically similar.

4 RESULTS AND DISCUSSION

This chapter presents the findings and analysis of isothermal interdiffusion experiments conducted for a Cu-Ni system. The results consist of the plots of $\widetilde{D}$(C) and D_{ave}. The *p-values* are also given, which allows for a statistical comparison between the different experimental conditions.

4.1 Experimental Verification of Effect of Time in Cu-Ni System

The verification of the effect of time on $\widetilde{D}$(C) is done by comparing the results for isothermal treatments for different time intervals. The temperatures used in this study are 900°C, 950°C and 1000°C and the time intervals are 5-25 hours, 25-75 hours, and 75-150 hours.

4.1.1 Experimental Verification of Effect of Time in Cu-Ni System at 900°C

The experimental concentration profiles for the diffusion couples with the pure element system are presented in Figures 4.1. The interdiffusion coefficients for concentrations that range from 5 to 95 at% Cu for all time intervals are given in Figures 4.2 to 4.4. Observing the $\widetilde{D}$ (C) curves, it is clear that the interdiffusion coefficients are changing as the diffusion time changes, especially comparing the shortest and longest diffusion times (Figure 4.4) for which there is virtually no overlap of the plots and the error bars. Table 4.1 shows the *p*-values for the comparison of all time intervals, the boxes highlighted in red show the values above the 0.5 threshold that represent statistical similarity. Most of the values are below 0.001, which is significantly lower than the threshold of 0.05, thus indicating that the interdiffusion coefficients are statistically different. Therefore, the interdiffusion coefficient of the Cu-Ni system varies with time at 900°C. In terms of the trend, the interdiffusion coefficient curves tend to differ more significantly in the Cu-rich side, and the *p*-values seem to decrease as the Cu content increases. This tendency will be further investigated for the other temperatures (950°C and 1000°C) in the next sections.

Table 4.2 presents the D_{ave} for the different time intervals, as well as their percentage differences. The average diffusivity decreases 120% with longer time intervals; that is, from 5-25 h to 75-150 h. Overall, the changes of the interdiffusion coefficient curves and average diffusivity in this experiment contradict the general assumptions in the literature, as the interdiffusion coefficient does isothermally vary with diffusion time at 900°C.

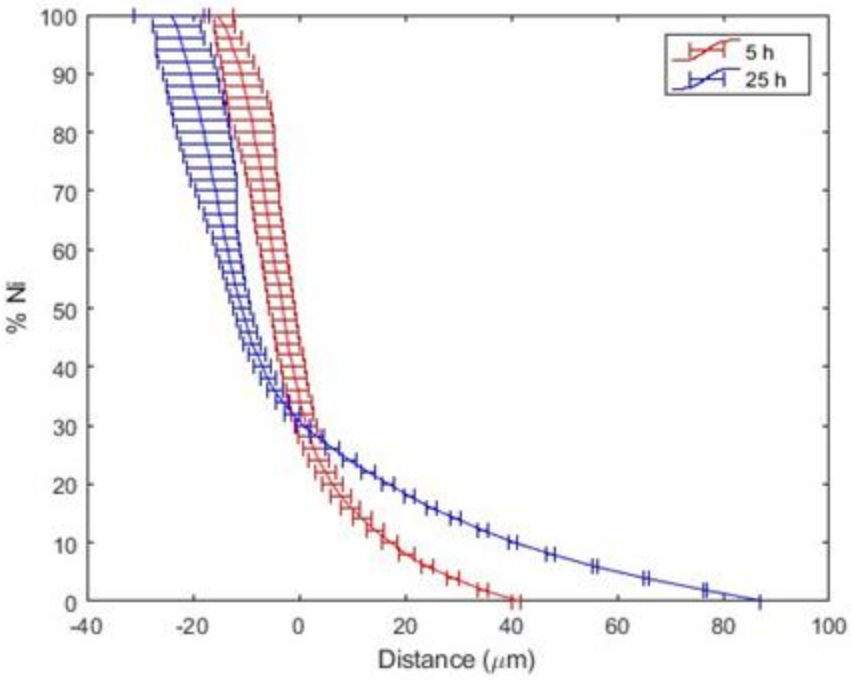

(a)

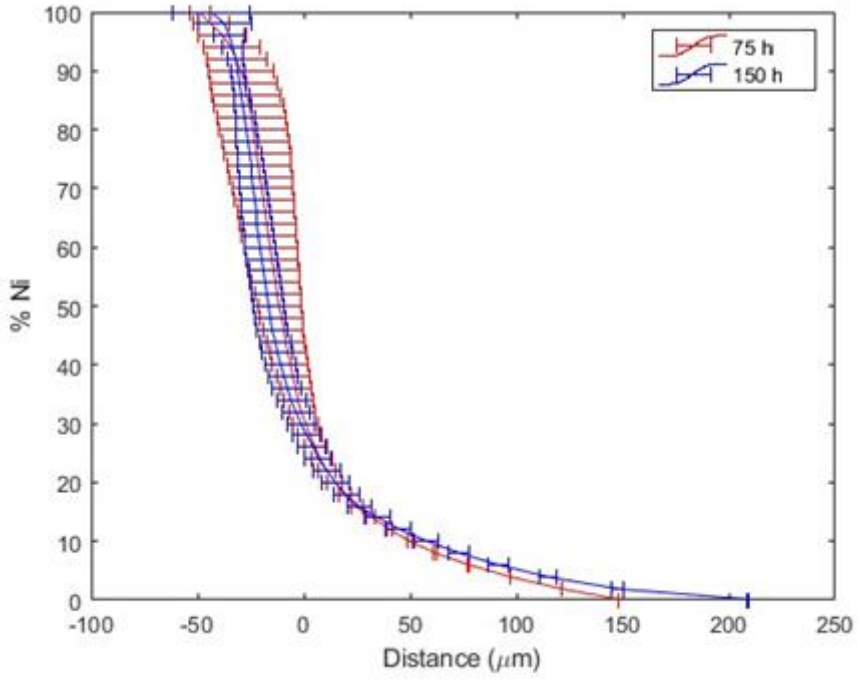

(b)

Figure 4.1. Concentration profiles for (a) 5 and 25 hours and (b) 75 and 150 hours

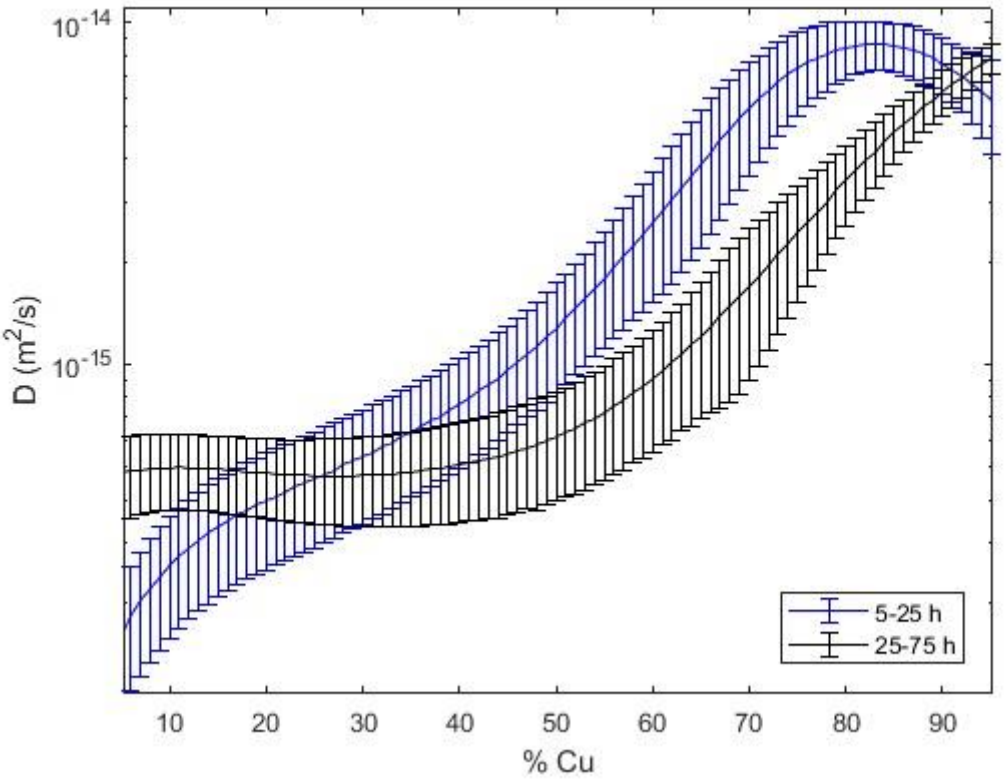

Figure 4.2. Interdiffusion coefficients of Cu-Ni system at 900°C for 5-25 hours and 25-75 hours

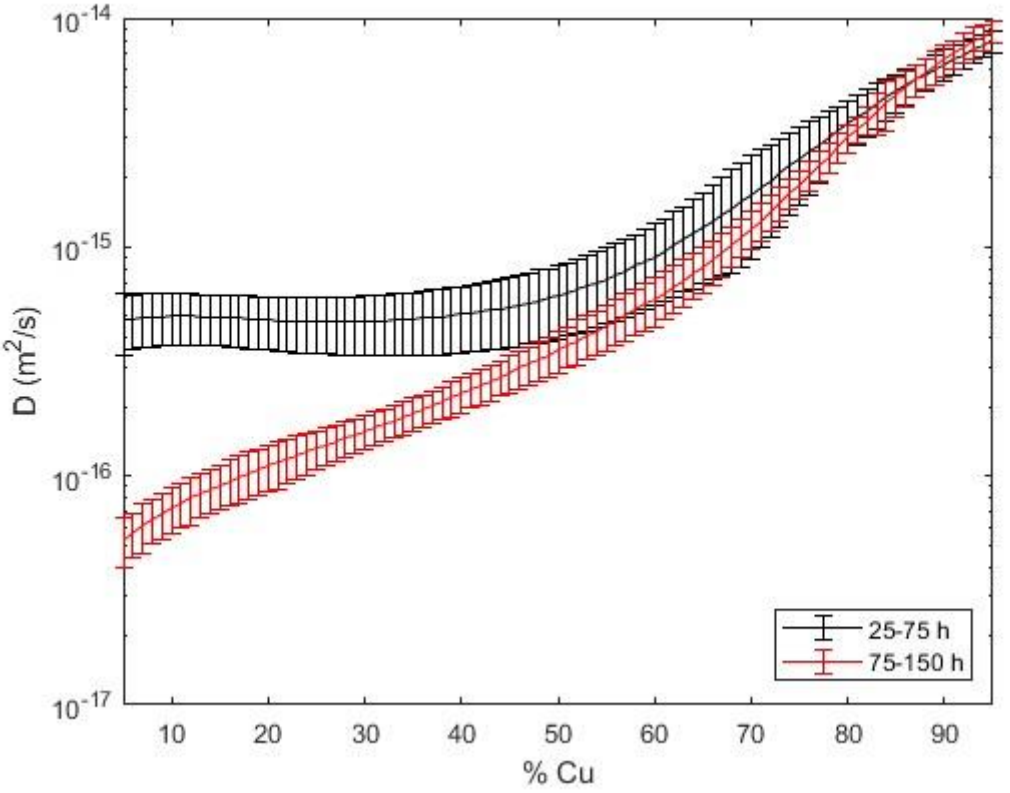

Figure 4.3. Interdiffusion coefficients of Cu-Ni system at 900°C for 25-75 hours and 75-150 hours

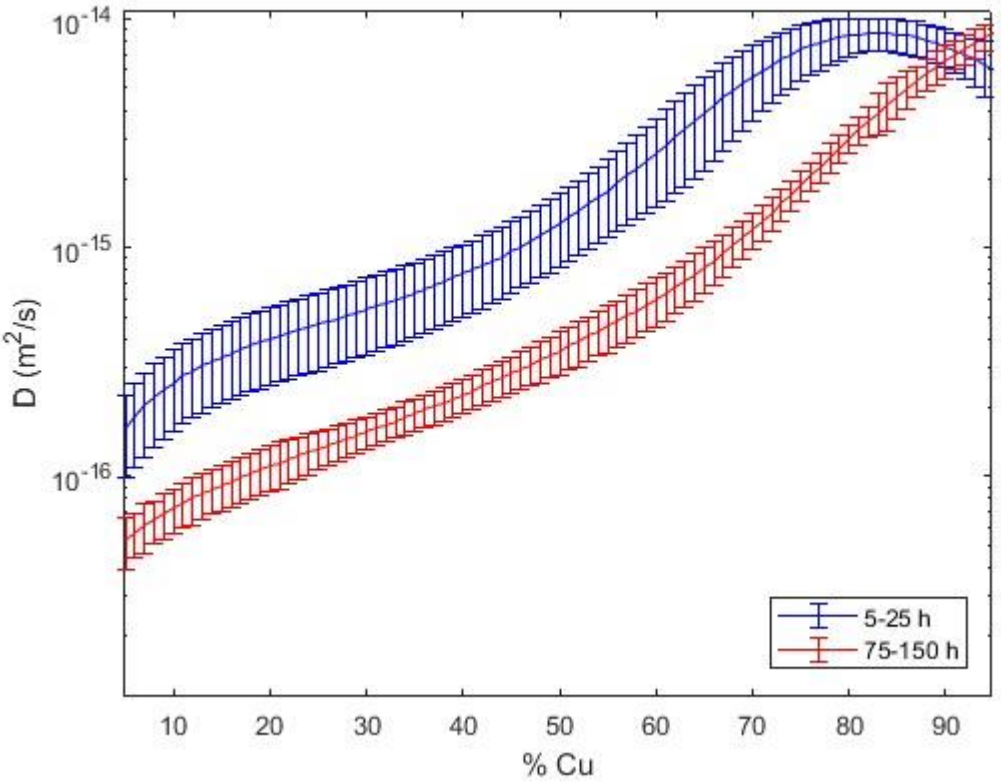

Figure 4.4. Interdiffusion coefficients of Cu-Ni system at 900°C for 5-25 hours and 75-150 hours

Table 4.1. *p-values* of Cu-Ni system at 900°C

Cu at. %	**5.0**	**10.0**	**15.0**	**20.0**	**25.0**
5-25 h vs 25-75 h	0.007	0.537	0.349	0.031	0.002
5-25 h vs 75-150 h 25-75 h vs 75-150 h	< 0.001	< 0.001	< 0.001	< 0.001	< 0.001
Cu at. %	**30.0**	**35.0**	**40.0**	**45.0**	**50.0**
5-25 h vs 25-75 h 5-25 h vs 75-150 h 25-75 h vs 75-150 h	< 0.001	< 0.001	< 0.001	< 0.001	< 0.001
Cu at. %	**55.0**	**60.0**	**65.0**	**70.0**	**75.0**
5-25 h vs 25-75 h 5-25 h vs 75-150 h	< 0.001	< 0.001	< 0.001	< 0.001	< 0.001
25-75 h vs 75-150 h		0.005	0.013	0.019	
Cu at. %	**80.0**	**85.0**	**90.0**	**95.0**	
5-25 h vs 25-75 h 5-25 h vs 75-150 h	< 0.001	< 0.001	< 0.001	0.036 < 0.001	
25-75 h vs 75-150 h		0.003			

Table 4.2. Average diffusivity of Cu-Ni system at 900°C

Time (h)	$\boldsymbol{D_{ave}}$ (m^2/s)	% deviation from 5-25 h	*p*-value	% deviation from 25-75 h	*p*-value	% deviation from 75-150 h	*p*-value
5-25 h	3.038E-15	-	-	82%	< 0.001	120%	< 0.001
25-75 h	1.672E-15	45%	< 0.001	-	-	21%	< 0.001
75-150 h	1.383E-15	54%	< 0.001	17%	< 0.001	-	-

4.1.2 Experimental Verification of Effect of Time in Cu-Ni System at 950°C

In this study, the second temperature chosen for the interdiffusion experiment is 950°C. The plotted interdiffusion coefficients with Cu concentration for all time intervals at 950°C are presented in Figures 4.5 to 4.7. The D_{ave} and a percentage comparison for the different time periods are given in Table 4.4.

The $\widetilde{D}(C)$ curves show a significant overlap of the error bars for all of the time period comparisons throughout the entire concentration range, except for the points between 10 and 20% at. Cu for the time intervals of 5-25 hours and 25-75 hours, and below 10 % at. Cu for the time intervals of 25-75 hours and 75-150 hours. The p-values presented in Table 4.3 agree with this observation, in which the interdiffusion coefficients are seen to be statistically different ($p < 0.001$) for the comparisons and concentrations previously described. Additionally, it is worth noting that the interdiffusion coefficient is mostly statistically similar towards the Cu-rich side of the concentration range.

Table 4.3 provides further evidence of a time effect on the interdiffusion coefficient. D_{ave} is increased 19% from 5-25 hours to 25-75 hours. This increase is higher than the empirically determined error percentage of 15%.

In general, the influence of time on the interdiffusion coefficient in the Cu-Ni system at 950°C is evident, albeit not as pronounced as that observed for 900°C. This effect is primarily found within a limited concentration range at this temperature. Further investigations for 1000°C will be discussed in the next section.

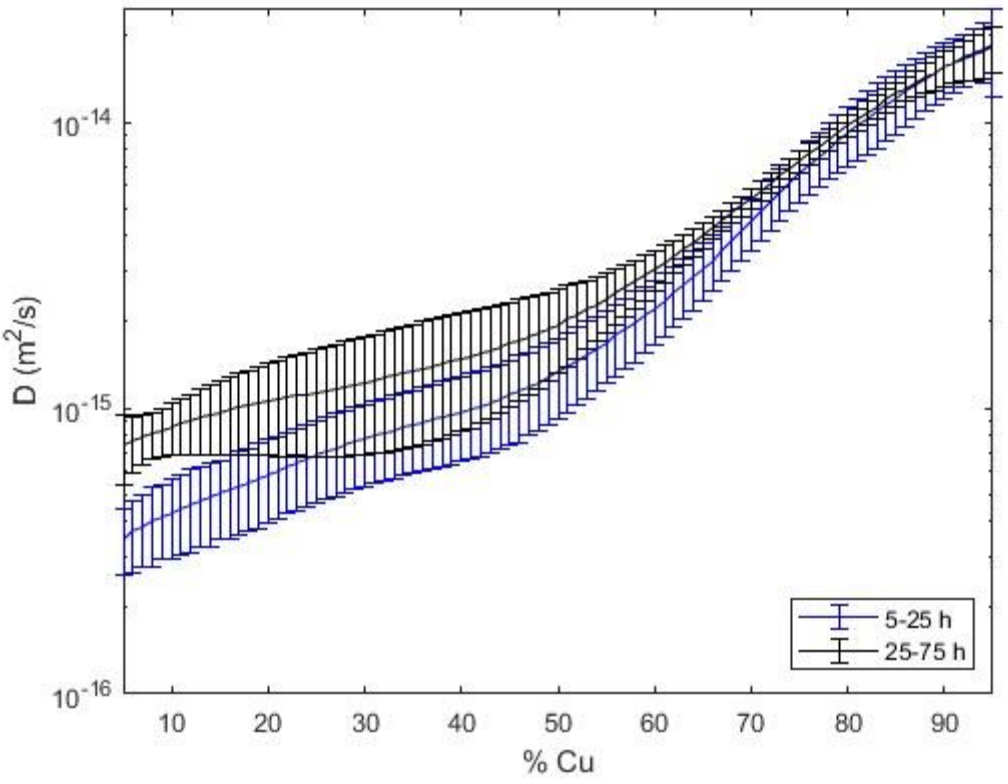

Figure 4.5. Interdiffusion coefficients of Cu-Ni system at 950°C for 5-25 hours and 25-75 hours

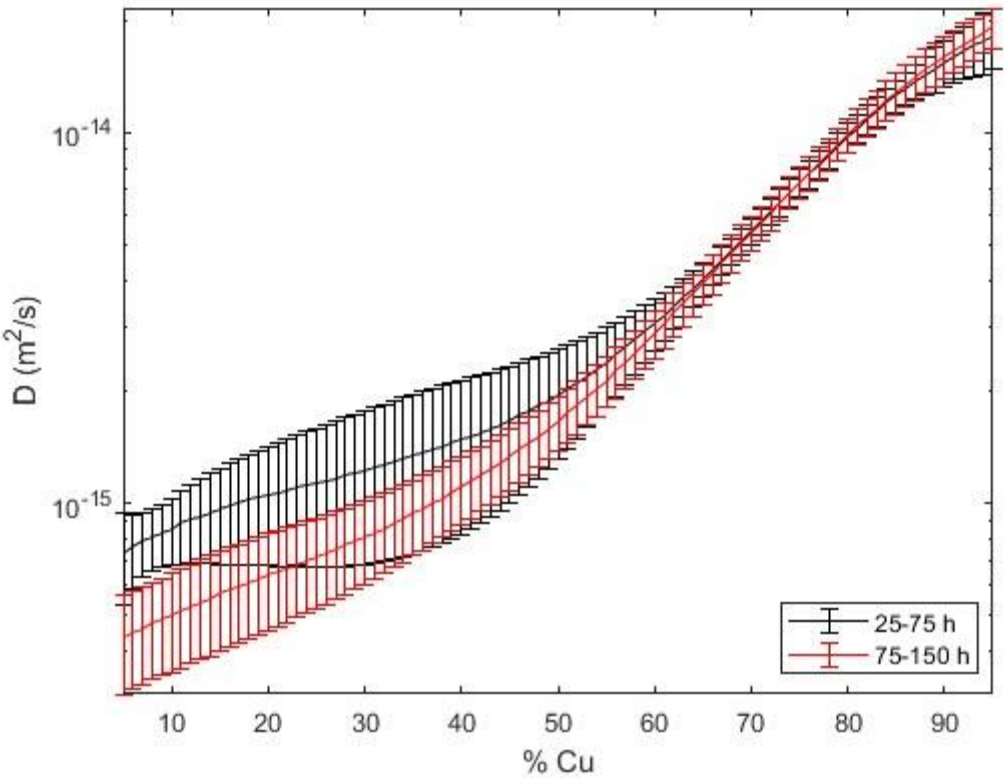

Figure 4.6. Interdiffusion coefficients of Cu-Ni system at 950°C for 25-75 hours and 75-150 hours

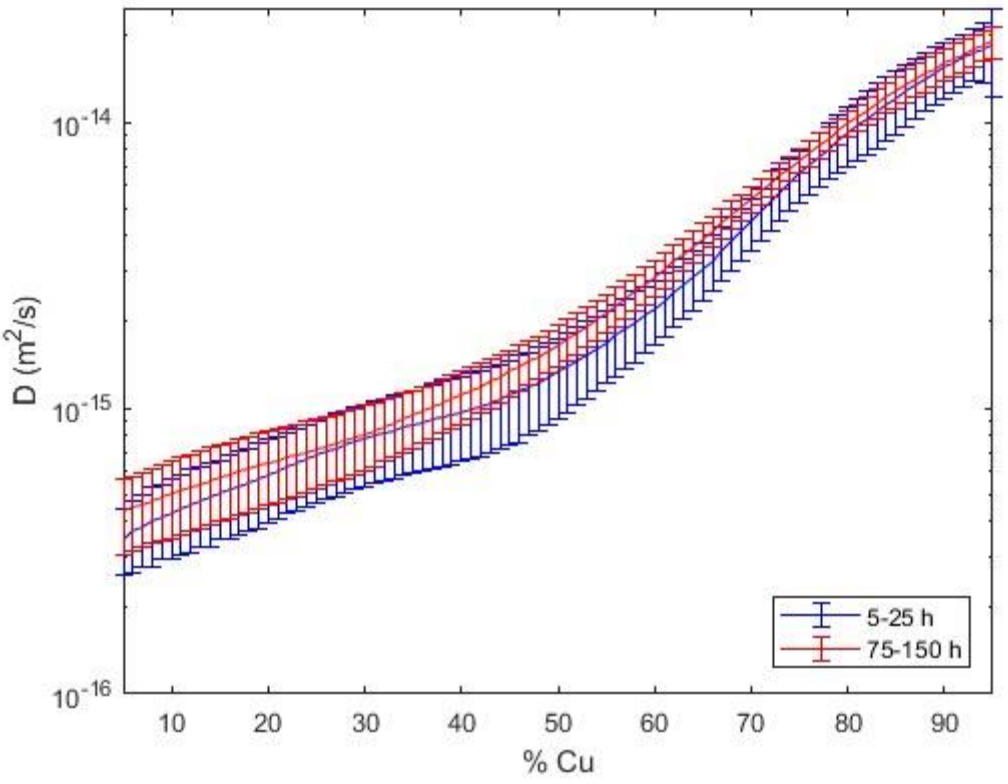

Figure 4.7. Interdiffusion coefficients of Cu-Ni system at 950°C for 5-25 hours and 75-150 hours

Table 4.3. *p*-values of Cu-Ni system at 950°C

Cu at. %	**5.0**	**10.0**	**15.0**	**20.0**	**25.0**
5-25 h vs 25-75 h	< 0.001	< 0.001	< 0.001	< 0.001	< 0.001
5-25 h vs 75-150 h	0.004	0.014	0.028	0.038	0.084
25-75 h vs 75-150 h	< 0.001	< 0.001	< 0.001	< 0.001	< 0.001
Cu at. %	**30.0**	**35.0**	**40.0**	**45.0**	**50.0**
5-25 h vs 25-75 h	< 0.001	< 0.001	< 0.001	< 0.001	< 0.001
5-25 h vs 75-150 h	0.095	0.041	0.010	0.002	0.001
25-75 h vs 75-150 h	< 0.001	< 0.001	< 0.001	< 0.001	< 0.001
Cu at. %	**55.0**	**60.0**	**65.0**	**70.0**	**75.0**
5-25 h vs 25-75 h				< 0.001	< 0.001
5-25 h vs 75-150 h	< 0.001	< 0.001	< 0.001	0.010	> 0.100
25-75 h vs 75-150 h				0.087	
Cu at. %	**80.0**	**85.0**	**90.0**	**95.0**	
5-25 h vs 25-75 h	0.021	0.078			
5-25 h vs 75-150 h	> 0.100	> 0.100	> 0.100	> 0.100	
25-75 h vs 75-150 h					

Table 4.4. Average diffusivity of Cu-Ni system at 950°C

Time (h)	$\boldsymbol{D_{ave}}$ (m^2/s)	% deviation from 5-25 h	*p*-value	% deviation from 25-75 h	*p*-value	% deviation from 75-150 h	*p*-value
5-25 h	3.975E-15	-	-	16%	< 0.001	8%	0.022
25-75 h	4.725E-15	19%	< 0.001	-	-	9%	< 0.001
75-150 h	4.345E-15	9%	0.022	8%	< 0.001	-	-

4.1.3 Experimental Verification of Effect of Time in Cu-Ni System at 1000°C

This section discusses the interdiffusion analysis for the Cu-Ni system at 1000°C. The plotted interdiffusion coefficients with Cu concentration for all time intervals are given in Figures 4.8 to 4.10. In Table 4.6, the $D_{ave}s$ are shown for all time intervals, and the percentage variations between these averages are calculated and presented.

A closer examination of the $\widetilde{D}(C)$ curves reveals distinct trends, mostly associated with the Cu-rich side of the concentration range. The error bars show very little overlap towards the 70 at. % Cu to 100 at. % Cu range for the compared time intervals of 5-25 hours and 25-75 hours as well as 5-25 hours and 75-150 hours. For the compared time intervals of 25-75 hours and 75-150 hours, however, the curves are mostly different at the Ni-rich side up to 40 % at. Cu.

The statistical significance of these observations is quantified by using *p-values*, as shown in Table 4.5. The data suggest that the majority of the interdiffusion coefficient values for all of the time comparisons are mostly statistically different, with some isolated exceptions. As seen in Table 4.6, D_{ave} shows a gradual reduction as the annealing time increases. D_{ave} decreases by 15% as the time range increases from 5-25 hours to 25-75 hours, and further decreases to 30% as the time range reaches 75-150 hours. The deviation between the two first time intervals is not above the error margin of 15%, which is also the case for the comparison of the time intervals of 25-75 hours and 75-150 hours.

Overall, a time effect on the interdiffusion coefficients is also present in the Cu-Ni system at 1000°C. This influence is more evident by comparing the shortest and longest annealing times.

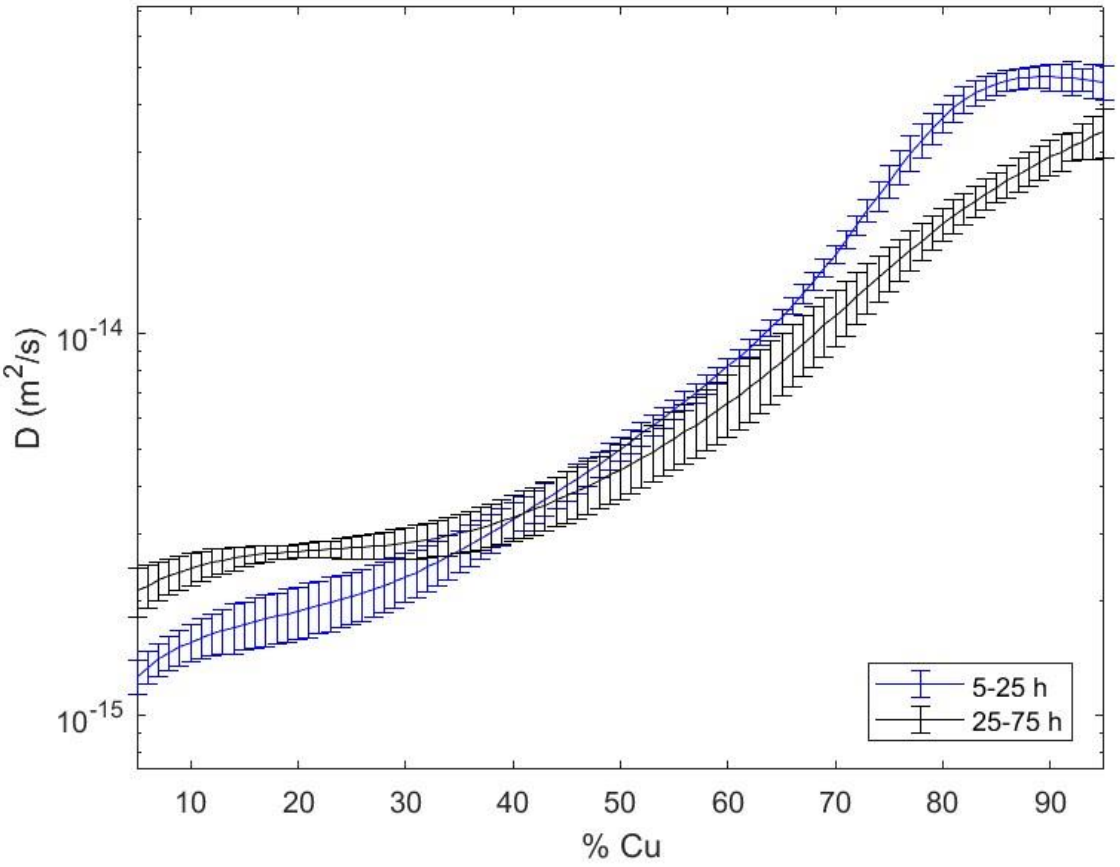

Figure 4.8. Interdiffusion coefficients of Cu-Ni system at 1000°C for time intervals of 5-25 hours and 25-75 hours

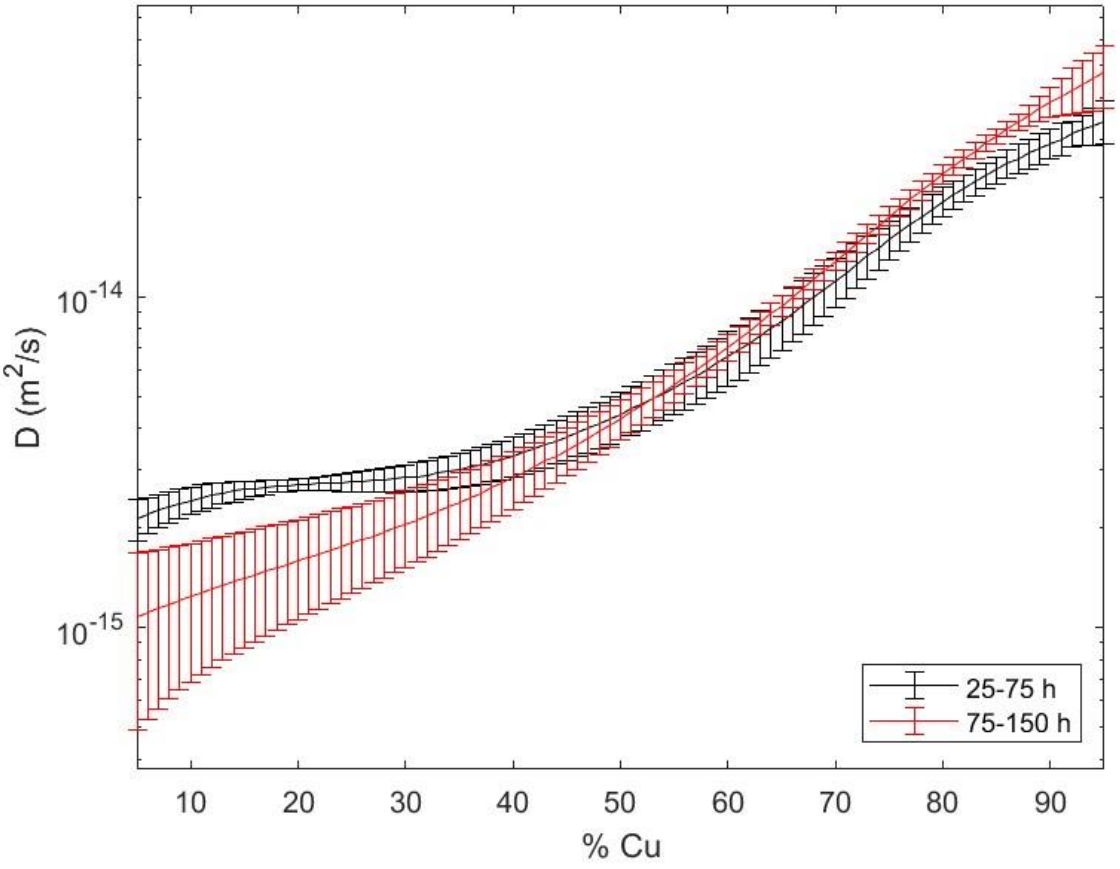

Figure 4.9. Interdiffusion coefficients of Cu-Ni at 1000 °C for 25-75 hours and 75-150 hours

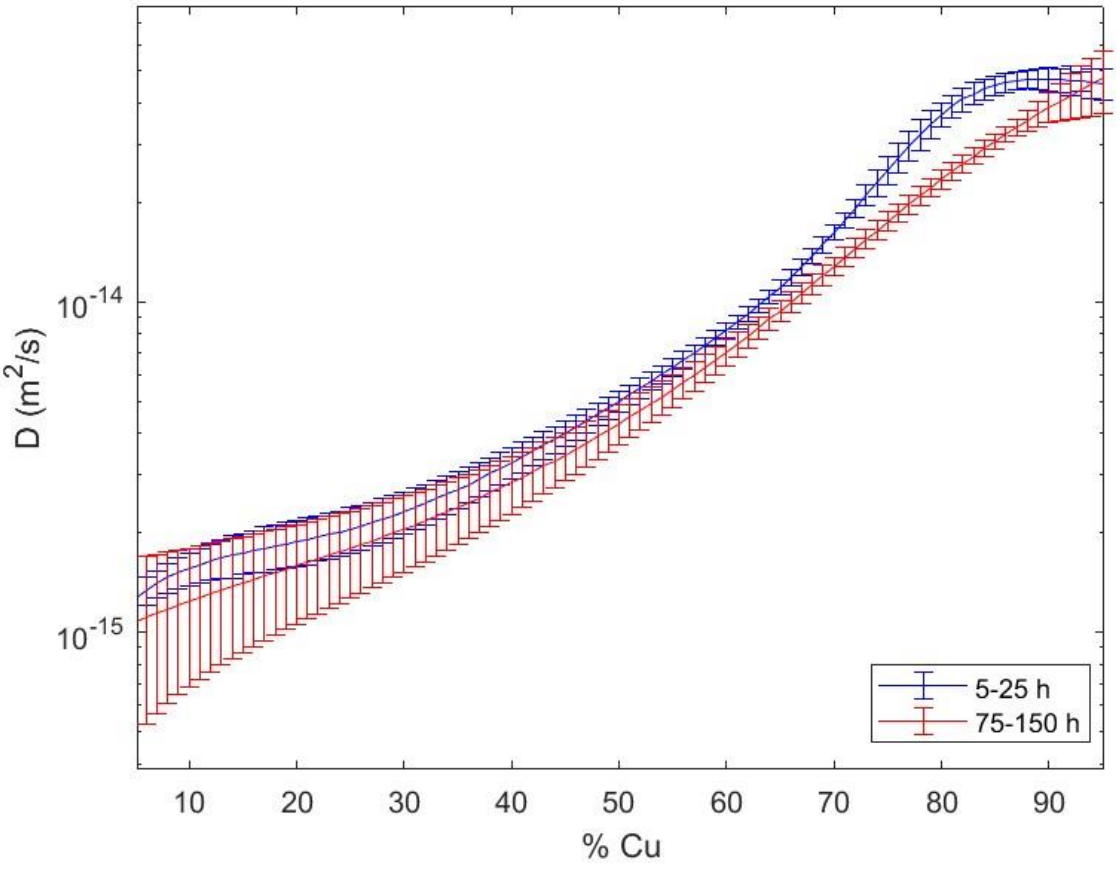

Figure 4.10. Interdiffusion coefficients of Cu-Ni system at 1000°C for 5-25 hours and 75-150 hours

Table 4.5. *p*-values of Cu-Ni system at 1000°C

Cu at. %	**5.0**	**10.0**	**15.0**	**20.0**	**25.0**
5-25 h vs 25-75 h	< 0.001				
5-25 h vs 75-150 h	0.030	< 0.001	< 0.001	< 0.001	< 0.001
25-75 h vs 75-150 h	< 0.001				
Cu at. %	**30.0**	**35.0**	**40.0**	**45.0**	**50.0**
5-25 h vs 25-75 h					0.09
5-25 h vs 75-150 h	< 0.001	< 0.001	< 0.001	< 0.001	
25-75 h vs 75-150 h					< 0.001
Cu at. %	**55.0**	**60.0**	**65.0**	**70.0**	**75.0**
5-25 h vs 25-75 h	0.03	< 0.001	< 0.001	< 0.001	< 0.001
5-25 h vs 75-150 h	< 0.001				
25-75 h vs 75-150 h		0.074	0.706	0.390	0.207
Cu at. %	**80.0**	**85.0**	**90.0**	**95.0**	
5-25 h vs 25-75 h	< 0.001				
5-25 h vs 75-150 h		< 0.001	< 0.001	< 0.001	
25-75 h vs 75-150 h	0.090				

Table 4.6. Average diffusivity of Cu-Ni system at 1000°C

Time (h)	$\boldsymbol{D_{ave}}$ (m^2/s)	% deviation from 5-25 h	*p*-value	% deviation from 25-75 h	*p*-value	% deviation from 75-150 h	*p*-value
5-25 h	1.362E-14	-	-	16 %	< 0.001	29 %	< 0.001
25-75 h	1.169E-14	15%	< 0.001	-	-	11 %	
75-150 h	1.053E-14	23 %	< 0.001	10 %	0.4	-	-

4.1.4 Summary of Experimental Verification of Effect of Time in Cu-Ni System

In this study, $\widetilde{D}$(C) varies with time for the Cu-Ni system at a temperature range of 900 to 1000°C. This finding contradicts the common assumption in the literature that interdiffusion coefficients do not depend on time. More specifically, the time effect is more pronounced in the Cu-rich regions of the concentration ranges and during the initial stages of diffusion. This effect is also more evident at 900°C.

Furthermore, the interdiffusion coefficient is seen to mostly decrease as the annealing time is increased for all temperatures. One exception are the results for the time interval of 25–75-hours at an annealing temperature of 950°C. Overall, the diffusion time is observed to influence the behavior of the interdiffusion coefficient for the experiments performed. This time effect can be related to the existence of DIS during diffusion, and this correlation will be discussed in the next section.

4.2 Time Effect and DIS

As previously discussed, the most likely cause of the changes of the interdiffusion coefficients with diffusion time is the DIS. The changes in the concentration gradient drive the diffusion process and the difference in the intrinsic fluxes causes the generation of internal stresses - DIS [18]. Consequently, the presence of DIS changes the diffusion mobility and results in variations in the interdiffusion coefficients [17]. This feedback loop, in turn, leads to the generation of more DIS. In summary, the concentration gradient changes lead to the generation of DIS, which subsequently leads to larger interdiffusion coefficients and more DIS. A schematic of this relationship is presented in Figure 4.11.

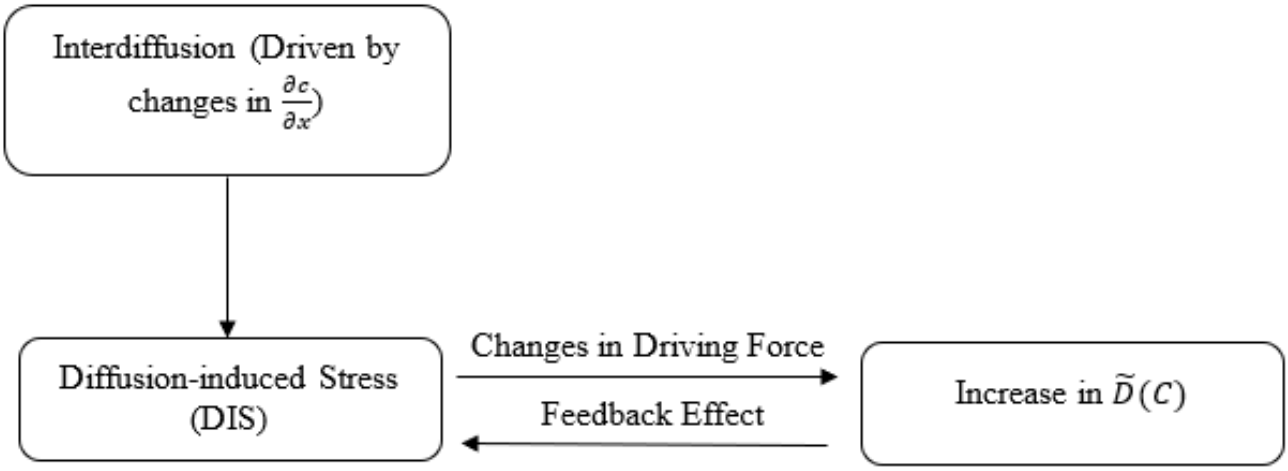

Figure 4.11. Relationship between interdiffusion and DIS.

Given the direct relationship between the changes in the concentration gradient and DIS, the concentration gradient in this study is used to modulate the DIS. As the concentration gradient evolves with diffusion time, the magnitude and presence of DIS will also change with time. In turn, these changes will be reflected in the interdiffusion coefficient. Therefore, if changes in the concentration gradient result in time-dependent variations of the interdiffusion coefficient, the DIS could be the underlying reason for this time effect.

In order to further validate the influence of concentration gradient changes on the interdiffusion coefficient, two different conditions were examined that involve the presence of an initial uniform and non-uniform solute distribution. These conditions are compared to the Cu-Ni system without the initial solute distribution prior to the diffusion treatment. The uniform solute distribution couples consist of pure Cu and a $Cu_{50}Ni_{50}$ alloy, while the non-uniform couples comprise pure Cu and pure Ni subjected to annealing prior to the diffusion treatment.

4.3 Experimental Verification of Influence of Initial Uniform Distribution of Solute

Verifying the influence of the initial uniform distribution of solute on $\widetilde{D}$(C) was done by comparing the results of the Cu-Ni system for the pure element and alloy couples. In the former, the starting materials are 100 at. % Cu and 100 at. % Ni, and for the latter, 50 at. % Ni and 100 at. % Cu. The following sections present the results for alloy couples at 900°C, 950°C and 1000°C for 5-25 hours, 25-75 hours, and 75-150 hours. The results are compared to those of the pure element couples as presented in Section 4.1.

4.3.1 Influence of Initial Uniform Distribution of Solute at 900°C

This section discusses the results of the interdiffusion coefficients of the Cu-Ni system with an initial uniform distribution of solute at 900°C. The interdiffusion coefficients of the systems without a pre-existing uniform solute distribution are compared to those with an initial uniform distribution of solute for concentrations that range from 55 to 95 at. % Cu for 5-25 hours, 25-75 hours and 75-150 hours. The curves are plotted in Figures 4.12 to 4.14.

The $\widetilde{D}(C)$ curves are predominantly similar in terms of the magnitude and error bar overlap for the two longest time intervals. For 5-25 hours, the curves only intersect on the Cu-rich side of the concentration spectrum (from 85 to 100 at. % Cu). Correspondingly, the *p*-values, as listed in Table 4.7, are in agreement with the trend of the interdiffusion curves. In comparing the time interval of 5-25 hours, a consistent statistical difference ($p < 0.001$) is seen throughout the entire concentration range, while for 25-75 hours and 75-150 hours, the values are mostly statistically similar.

Table 4.8 presents the D_{ave} of the systems with a pre-existing uniform solute distribution as well as a percentage deviation compared to the systems without an initial uniform distribution of solute

(previously discussed in Section 4.1.1). The D_{ave} of the Cu-Ni system is 63% higher than the diffusivity of the system with a pre-existing uniform solute distribution for 5-25 hours. For the other time intervals, the deviation does not exceed the error margin of 15%.

In general, the interdiffusion coefficient and average diffusivity are influenced by the concentration gradient changes resultant of the initial uniform distribution of solute. This challenges conventional assumptions that the interdiffusion coefficient remains the same for systems with and without an initial uniform distribution of solute.

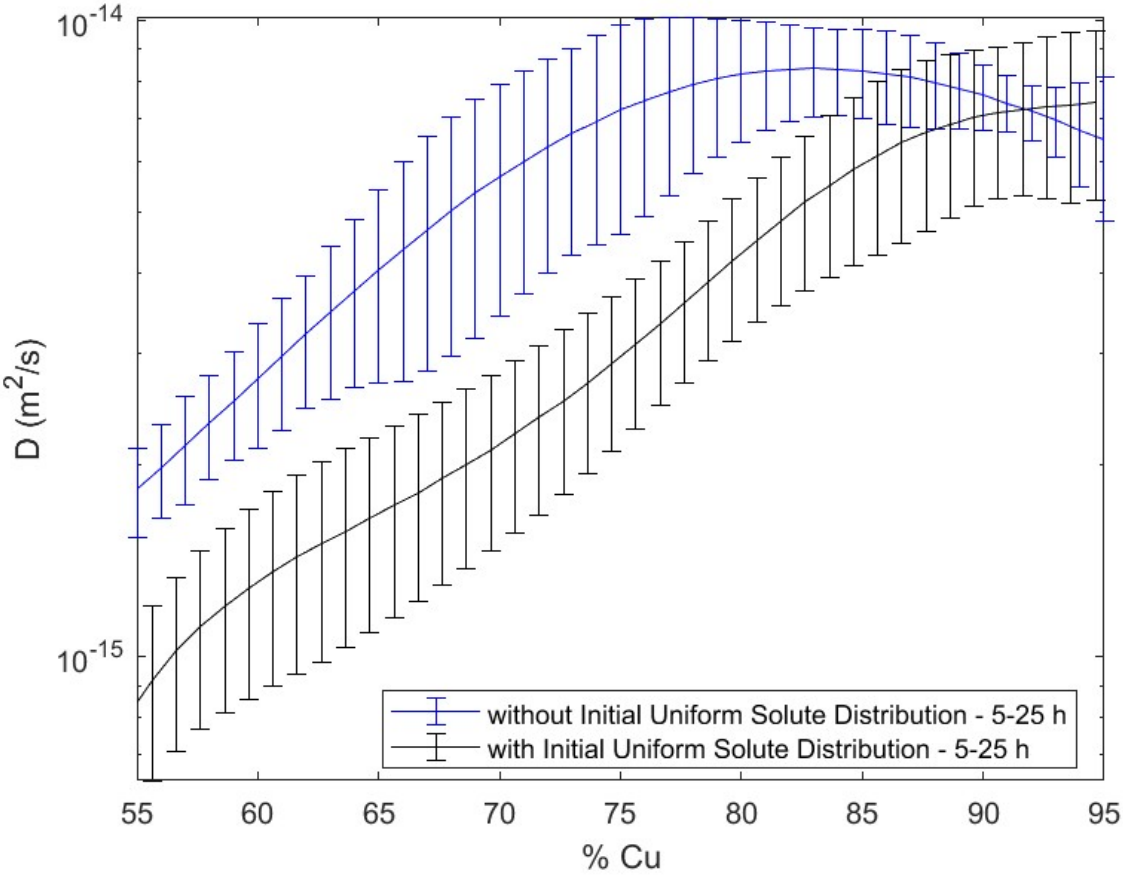

Figure 4.12. Interdiffusion coefficients of Cu-Ni systems with and without initial uniform distribution of solute at 900°C for 5-25 hours

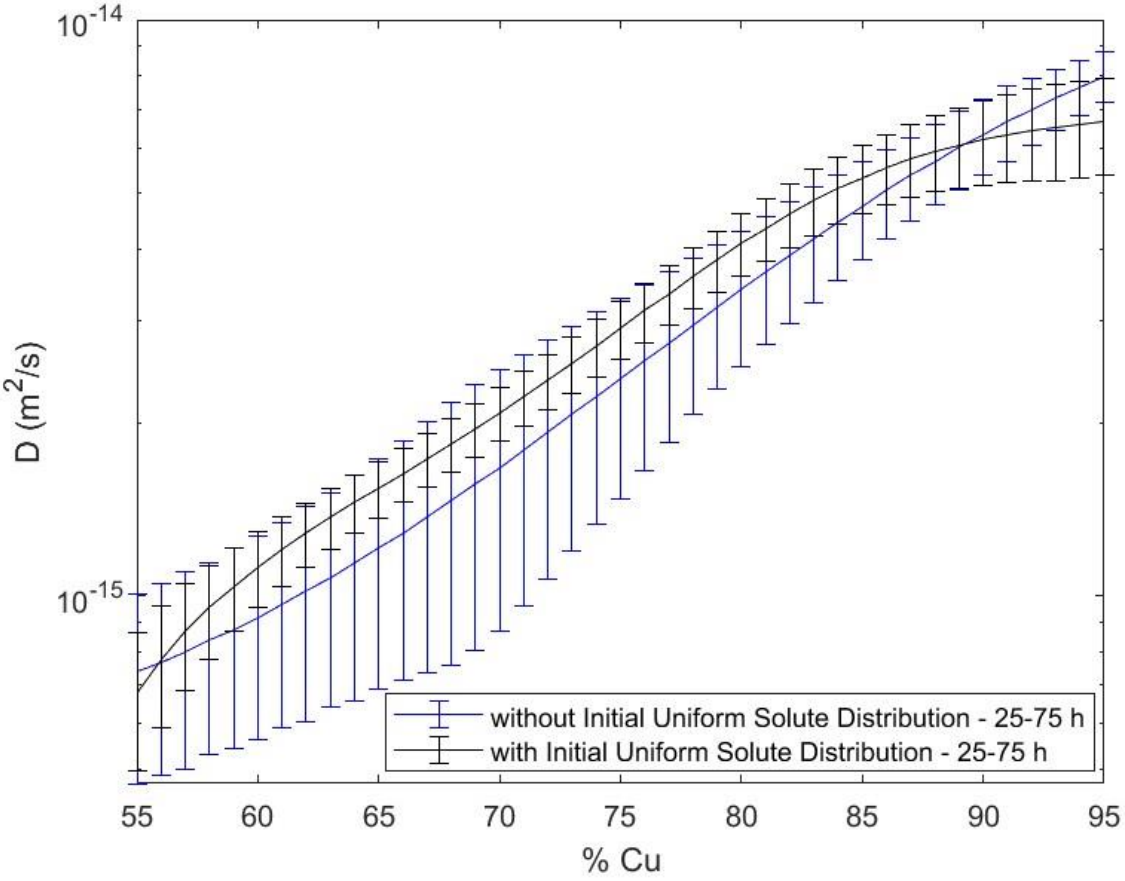

Figure 4.13. Interdiffusion coefficients of Cu-Ni systems with and without initial uniform distribution of solute at 900°C for 25-75 hours

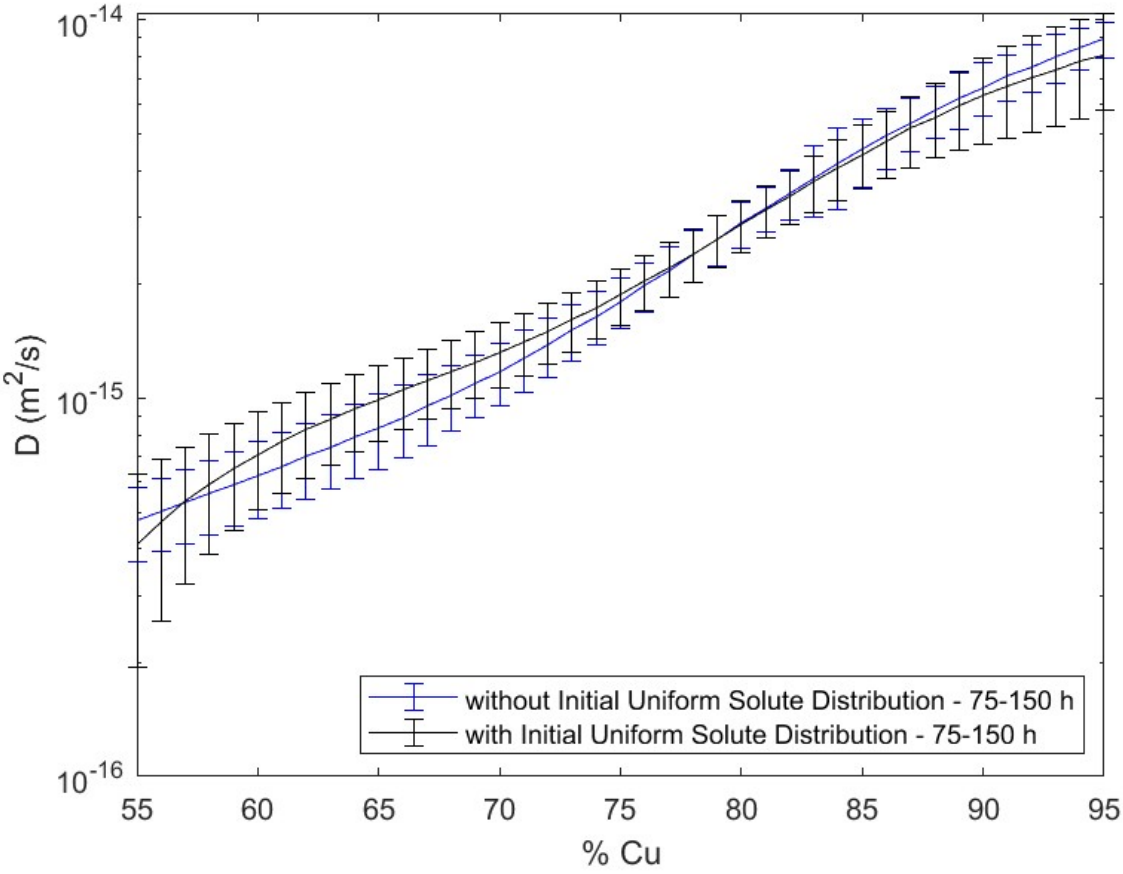

Figure 4.14. Interdiffusion coefficients of Cu-Ni systems with and without initial uniform distribution of solute at 900°C for 75-150 hours

Table 4.7. *p-values* of Cu-Ni systems with and without initial uniform distribution of solute at 900°C

Cu at. %	**55.0**	**60.0**	**65.0**	**70.0**	**75.0**
5-25 h	< 0.001	< 0.001	< 0.001	< 0.001	< 0.001
25-75 h	0.099	0.848	0.699	0.707	0.477
75-150 h	< 0.001	0.017	0.012	0.071	0.237
Cu at. %	**80.0**	**85.0**	**90.0**	**95.0**	
5-25 h	< 0.001	< 0.001	< 0.001	0.003	
25-75 h	0.689	0.635	0.454	0.045	
75-150 h	0.393	0.439	0.126	0.014	

Table 4.8. Average diffusivity of Cu-Ni systems with and without initial uniform distribution of solute at 900°C

Time (h)	$\boldsymbol{D_{ave}}$ (m^2/s) with Initial uniform distribution of solute	$\boldsymbol{D_{ave}}$ (m^2/s) No initial uniform distribution of solute	% difference	*p*-value
5-25 h	3.697E-15	6.025E-15	63%	< 0.001
25-75 h	3.377E-15	3.107E-15	8%	0.667
75-150 h	2.845E-15	2.955E-15	4%	0.118

4.3.2 Influence of Initial Uniform Distribution of Solute at 950°C

The interdiffusion coefficients for the concentration range of Cu are presented in Figures 4.15 to 4.17. Table 4.10 provides the values for D_{ave} and a percentage-based comparison between the two systems.

The $\widetilde{D}(C)$ curves for 5-25 hours and 75-150 hours are similar throughout the entire concentration spectrum. The error bars for the curves show no overlap for approximately 65 to 80 % at. Cu for 25-75 hours. These observations are statistically validated by the *p*-values in Table 4.9, which concur with the observed trends of the interdiffusion curves. The values are statistically different for the entire concentration range for 25-75 hours. Conversely, the remaining two time intervals are predominantly statistically similar.

The calculated average diffusivity of the system with an initial uniform distribution of solute is 19.% higher compared to the pure element system for 25–75-hours. The other comparisons remain within the designated error margin. Overall, similar to the system without a pre-existing uniform solute distribution, the extent of change of the interdiffusion coefficients appears to be less pronounced at 950°C in comparison to 900°C.

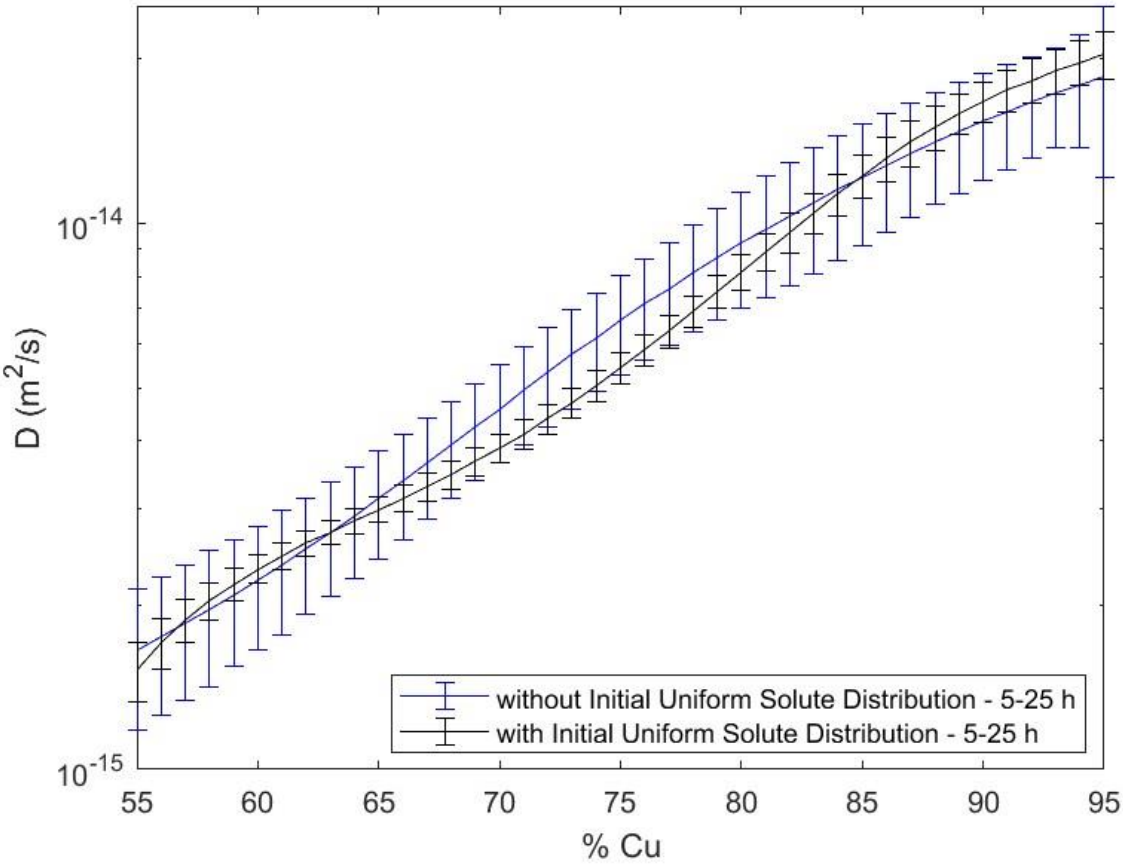

Figure 4.15. Interdiffusion coefficients of Cu-Ni systems with and without initial uniform distribution of solute at 950°C for 5-25 hours

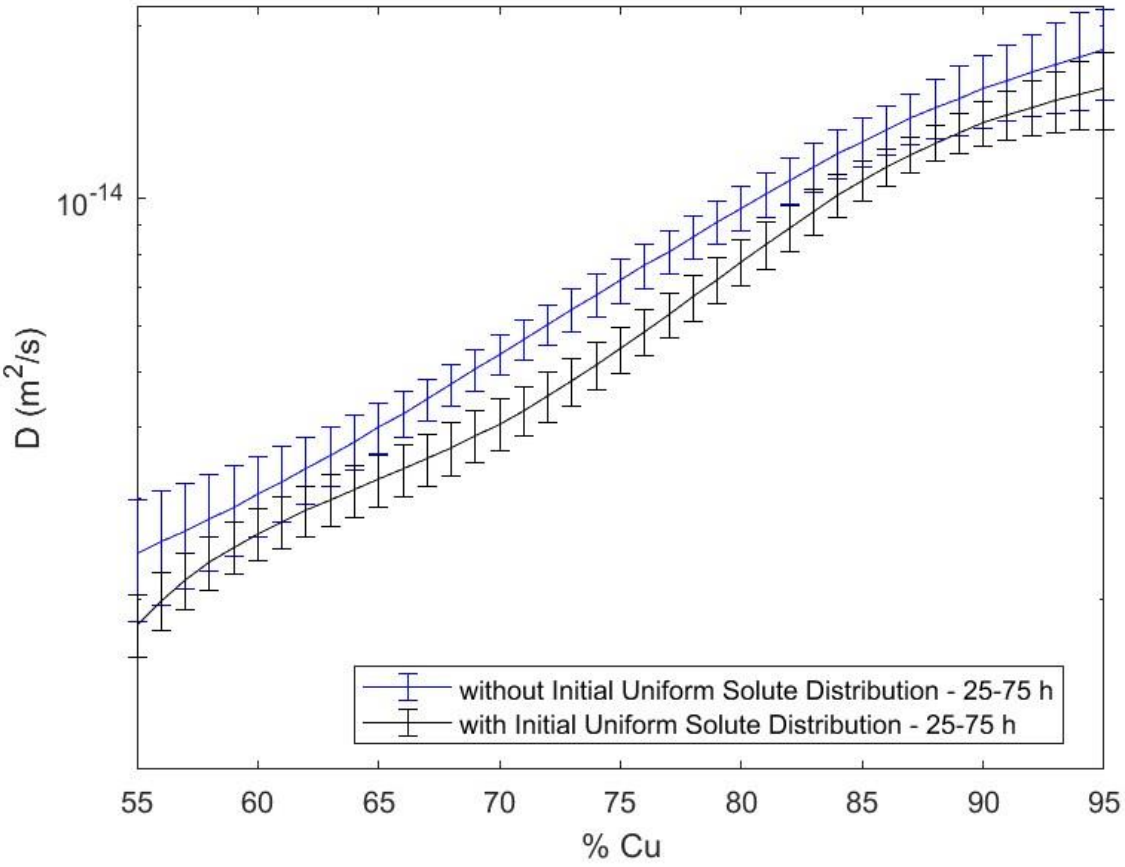

Figure 4.16. Interdiffusion coefficients of Cu-Ni systems with and without initial uniform distribution of solute at 950°C for 25-75 hours

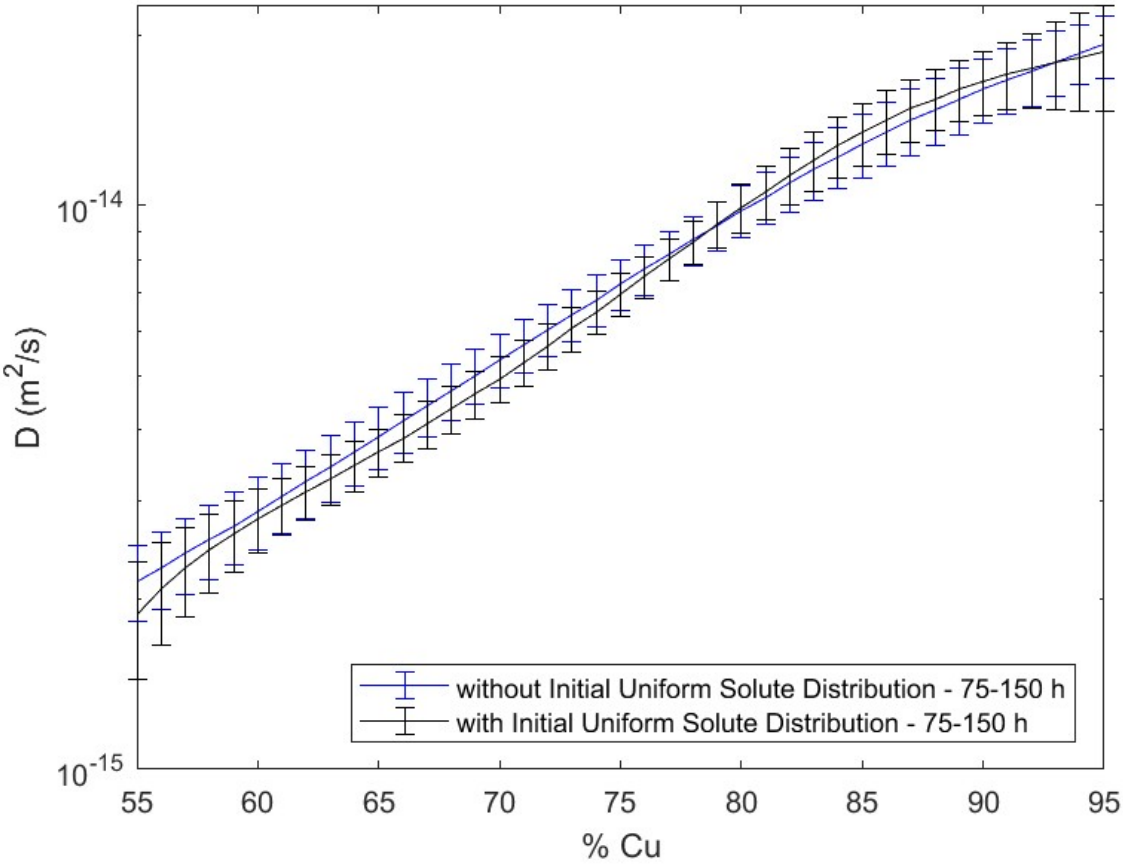

Figure 4.17. Interdiffusion coefficients of Cu-Ni systems with and without initial uniform distribution of solute at 950°C for 75-150 hours

Table 4.9. p-values of Cu-Ni systems with and without initial uniform distribution of solute at 950°C

Cu at. %	**55.0**	**60.0**	**65.0**	**70.0**	**75.0**
5-25 h	0.923	0.012	0.650	0.005	< 0.001
25-75 h	< 0.001	< 0.001	< 0.001	< 0.001	< 0.001
75-150 h	0.399	0.027	0.641	0.569	0.567
Cu at. %	**80.0**	**85.0**	**90.0**	**95.0**	
5-25 h	< 0.001	< 0.001	0.261	0.122	
25-75 h	< 0.001	< 0.001	< 0.001	0.033	
75-150 h	0.711	0.192	0.025	< 0.001	

Table 4.10. Average diffusivity of Cu-Ni systems with and without initial uniform distribution of solute at 950°C

Time (h)	$\boldsymbol{D_{ave}}$ (m^2/s) with Initial uniform distribution of solute	$\boldsymbol{D_{ave}}$ (m^2/s) No initial uniform distribution of solute	% difference	*p-value*
5-25 h	7.907E-15	7.884E-15	0.295 %	< 0.001
25-75 h	8.463E-15	7.083E-15	19 %	< 0.001
75-150 h	8.426E-15	8.537E-15	1 %	< 0.001

4.3.3 Influence of Initial Uniform Distribution of Solute at 1000°C

The interdiffusion coefficients curves for the concentration range of all time periods are given in Figures 4.18 to 4.20. The error bars for 5-25 hours and 25-75 hours do not overlap towards the Cu-rich side of the concentration spectrum. The plotted interdiffusion coefficients for the systems with and without a pre-existing uniform distribution of solute are comparable for the 75-150 hours time interval.

Table 4.11 presents the *p-values* for the three time intervals and shows that for the shorter time intervals, the interdiffusion coefficients are consistently statistically different from those of the systems without an initial uniform distribution of solute. However, most of the *p-values* for 75-150 hours are above the 0.05 threshold, thus indicating that the interdiffusion coefficients are statistically similar.

The average diffusivities, given in Table 4.12, show that the interdiffusion coefficient for the systems without an initial uniform distribution of solute exceeds the error margin in two instances. The difference is 36% for 5-25 hours, and 19% for 25-75 hours.

In general, a pre-existing uniform solute distribution changes the interdiffusion coefficient at 1000°C. This impact is more pronounced for shorter time intervals and notably towards the Cu-rich side of the concentration spectrum.

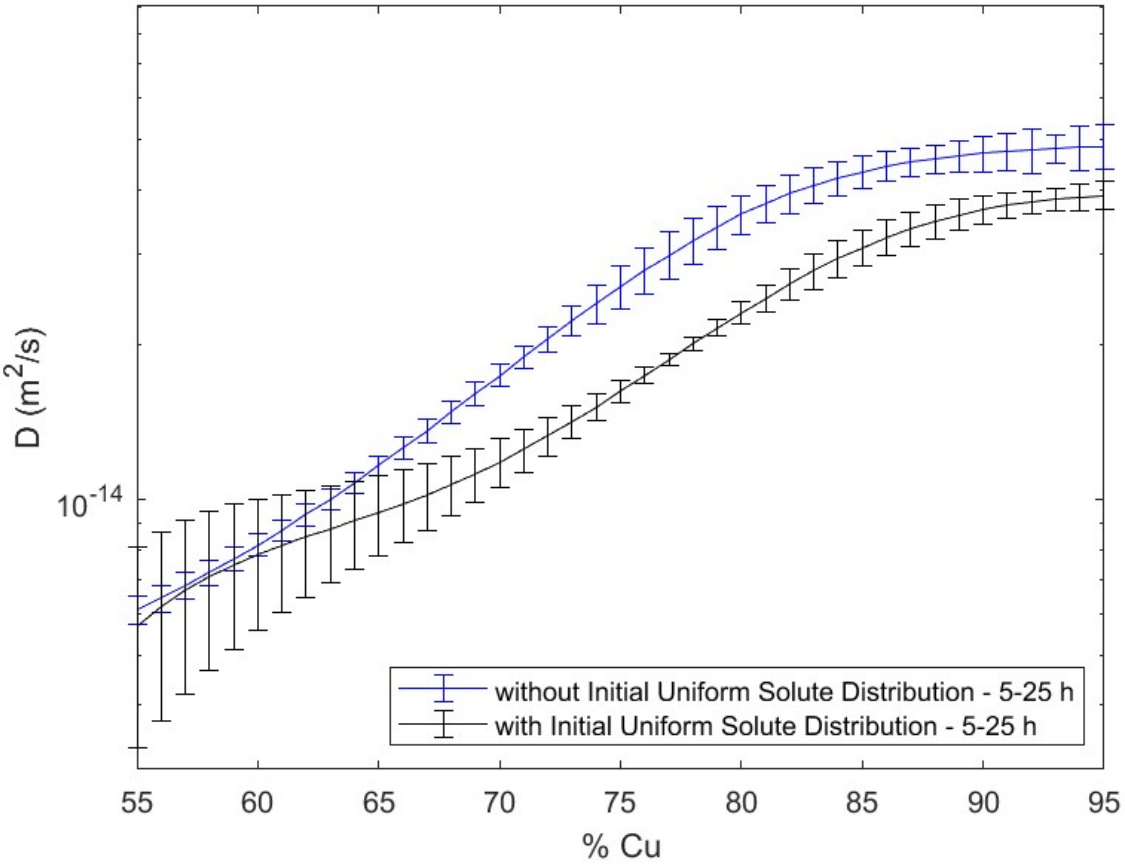

Figure 4.18. Interdiffusion coefficient of Cu-Ni systems with and without initial uniform distribution of solute at 1000°C for 5-25 hours

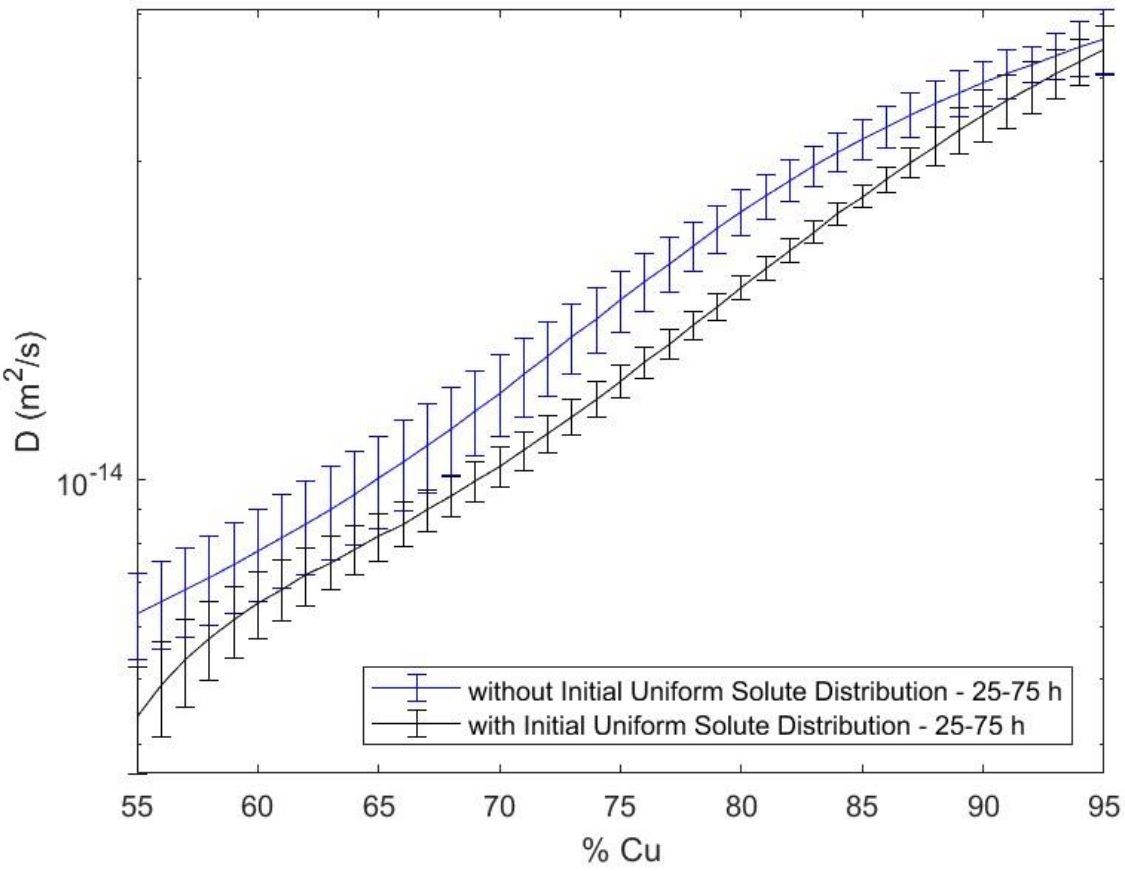

Figure 4.19. Interdiffusion coefficient of Cu-Ni systems with and without initial uniform distribution of solute at 1000°C for 25-75 hours

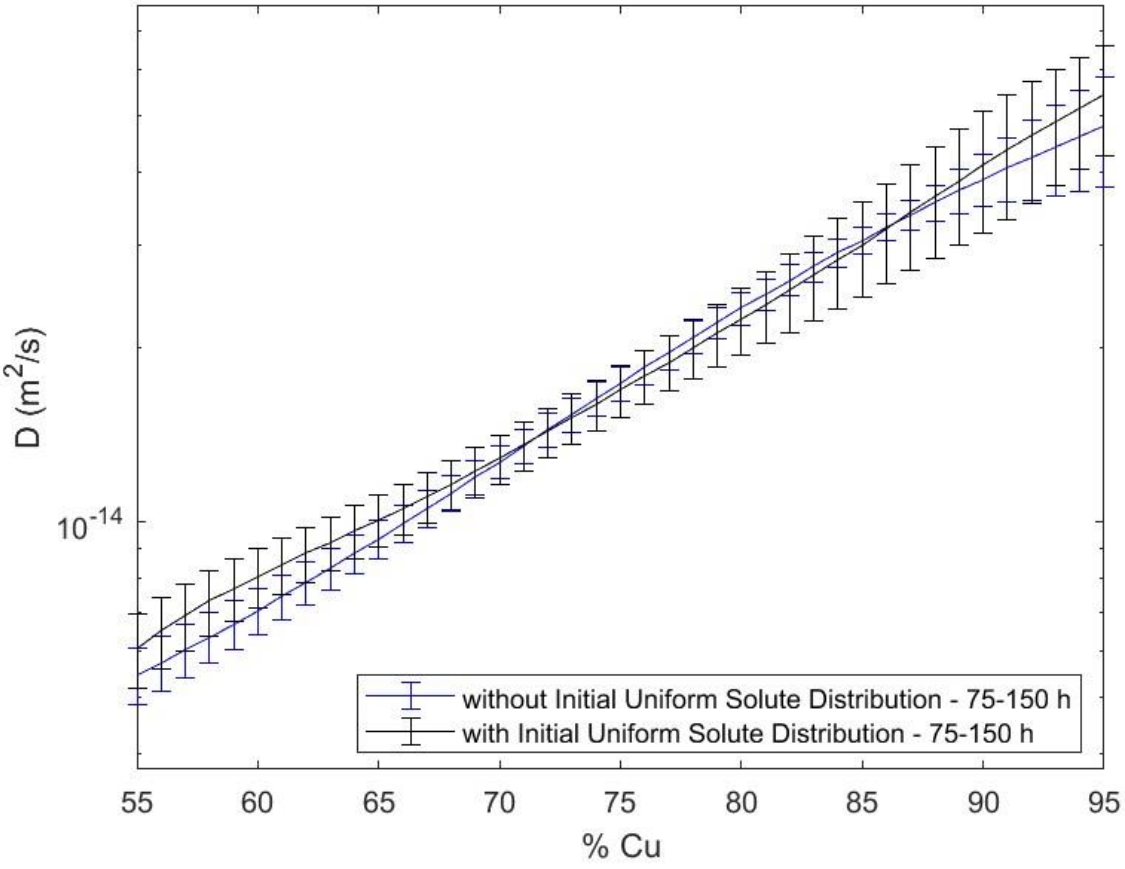

Figure 4.20. Interdiffusion coefficient of Cu-Ni systems with and without initial uniform distribution of solute at 1000°C for 75-150 hours

Table 4.11. *p*-values of Cu-Ni systems with and without initial uniform distribution of solute at 1000°C

Cu at. %	**55.0**	**60.0**	**65.0**	**70.0**	**75.0**
5-25 h	0.815	0.953	< 0.001	< 0.001	< 0.001
25-75 h	< 0.001	0.229	0.0694	< 0.001	< 0.001
75-150 h	0.084	0.055	0.011	0.912	0.072
Cu at. %	**80.0**	**85.0**	**90.0**	**95.0**	
5-25 h	< 0.001	< 0.001	< 0.001	< 0.001	
25-75 h	< 0.001	< 0.001	< 0.001	0.823	
75-150 h	0.062	< 0.001	< 0.001	< 0.001	

Table 4.12. Average diffusivity of Cu-Ni systems with and without initial uniform distribution of solute at 1000°C

Time (h)	$\boldsymbol{D_{ave}}$ (m^2/s) with Initial uniform distribution of solute	$\boldsymbol{D_{ave}}$ (m^2/s) No initial uniform distribution of solute	% difference	*p*-value
5-25 h	1.993E-14	2.711E-14	36 %	< 0.001
25-75 h	1.815E-14	2.162E-14	19 %	< 0.001
75-150 h	2.134E-14	2.062E-14	3 %	< 0.001

4.3.4 Summary of Experimental Verification of Influence of Initial Uniform Solute Distribution

In Section 4.3, $\widetilde{D}(C)$ was seen to change with the initial uniform distribution of solute for the Cu-Ni system at all temperatures. The concentration gradient changes induced by the initial uniform distribution of solute can be correlated to the presence of DIS. These effects are more obvious for the shortest diffusion times at 900°C.

The average interdiffusion coefficient difference between the pure element and alloy couples peaks at 63% at 900°C for 5-25 hours. The interdiffusion coefficient is higher for the pure element couple compared to the alloy couple. Interestingly, contrary to the pure element couples as discussed in Section 4.1.4, the interdiffusion coefficient does not decrease as the annealing time increases. The next section further investigates the influence of the concentration gradient on the interdiffusion coefficient by analyzing the results for the systems with an initial non-uniform distribution of solute.

4.4 Experimental Verification of Influence of Initial Non-uniform Distribution of Solute

Verifying the influence of a pre-existing non-uniform distribution of solute on concentration-dependent interdiffusion coefficients was done by comparing the results for the Cu-Ni system without an initial non-uniform distribution of solute at 950°C, that is, the system in Section 4.1.2, and the two systems for which an initial annealing treatment was performed. The first system, Type I, involving annealing in two stages: first at 900°C for 5 hours, then subsequently at 950°C for 5, 25, 75, and 150 hours. The second system, Type II, also involved the same annealing treatment with the only difference being the initial annealing temperature of 1000°C. The following sections present the results for Types I and II compared to the Cu-Ni system annealed in a single-stage at 950°C for 5-25 hours, 25-75 hours, and 75-150 hours.

4.4.1 Influence of Initial Non-uniform Distribution of Solute - Type I

The experimental concentration profiles for Type I and the single-stage Cu-Ni systems are given in Figure 4.21 for (a) 0, (b) 25, (c) 75, and (d) 150 hours. Without annealing (0 hours), the concentration profiles of the samples used in the single-stage systems were measured after electroplating. It can be observed that the concentration gradient difference decreases as the annealing time increases. There is a slight error bar overlap for the 0-hour profiles while at 150 hours, the profiles are nearly identical. The interdiffusion coefficients of concentrations that range from 5 to 95 % at. Cu for all time intervals are shown in Figures 4.22 to 4.25.

The $\widetilde{D}(C)$ curves show that the interdiffusion coefficient varies with an initial non-uniform distribution of solute, most significantly for the shortest annealing time and towards the Cu-rich side of the concentration spectrum. The D_{ave}s, presented in Table 4.14, show that the percentage difference is significant, and higher than 20%, for three of the four time intervals: 0-5 hours, 5-25 hours, and 75-150 hours, compared to the systems without an initial non-uniform distribution of solute, as shown in Table 4.14.

Despite the overlap of the error bars for 5-25 hours, the *p-values*, given in Table 4.13, demonstrate that the interdiffusion coefficient values are statistically different throughout most of the concentration range. Contrary to the other time intervals, the error bar overlap in the interdiffusion coefficient curves is seen on the Cu-rich side for 75-150 hours. The *p*-values for this time range show statistical similarity for Cu concentrations above 80 at. %.

Overall, the changes in the interdiffusion coefficient curves and D_{ave} seen in this experiment show that contrary to the assumptions in the literature, the interdiffusion coefficient is affected by the presence of an initial non-uniform distribution of solute.

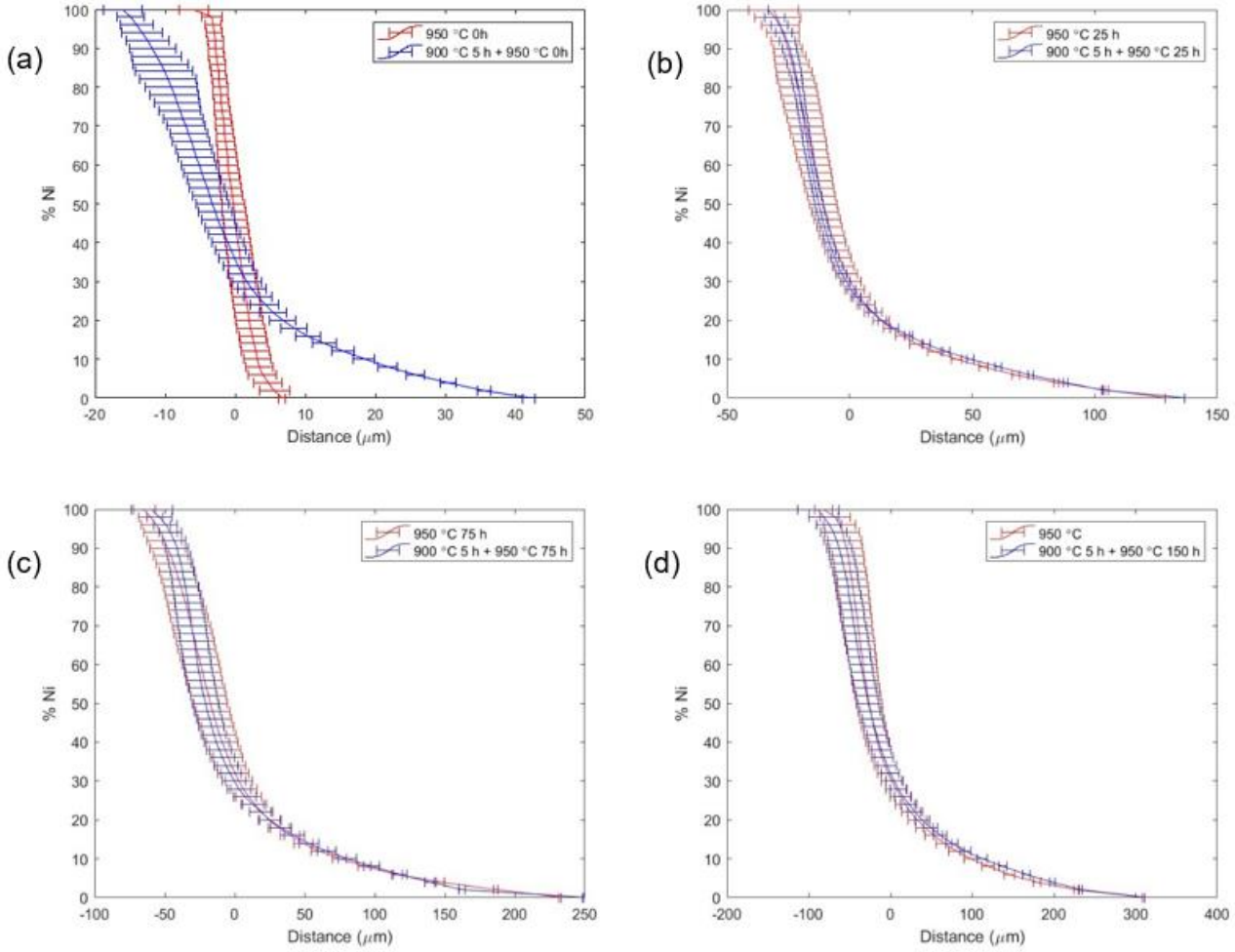

Figure 4.21. Experimental average concentration profiles for single-stage and multi-stage (Type I) treatments at 950°C for (a) 0 hour, (b) 25 hours, (c) 75 hours and (d) 150 hours

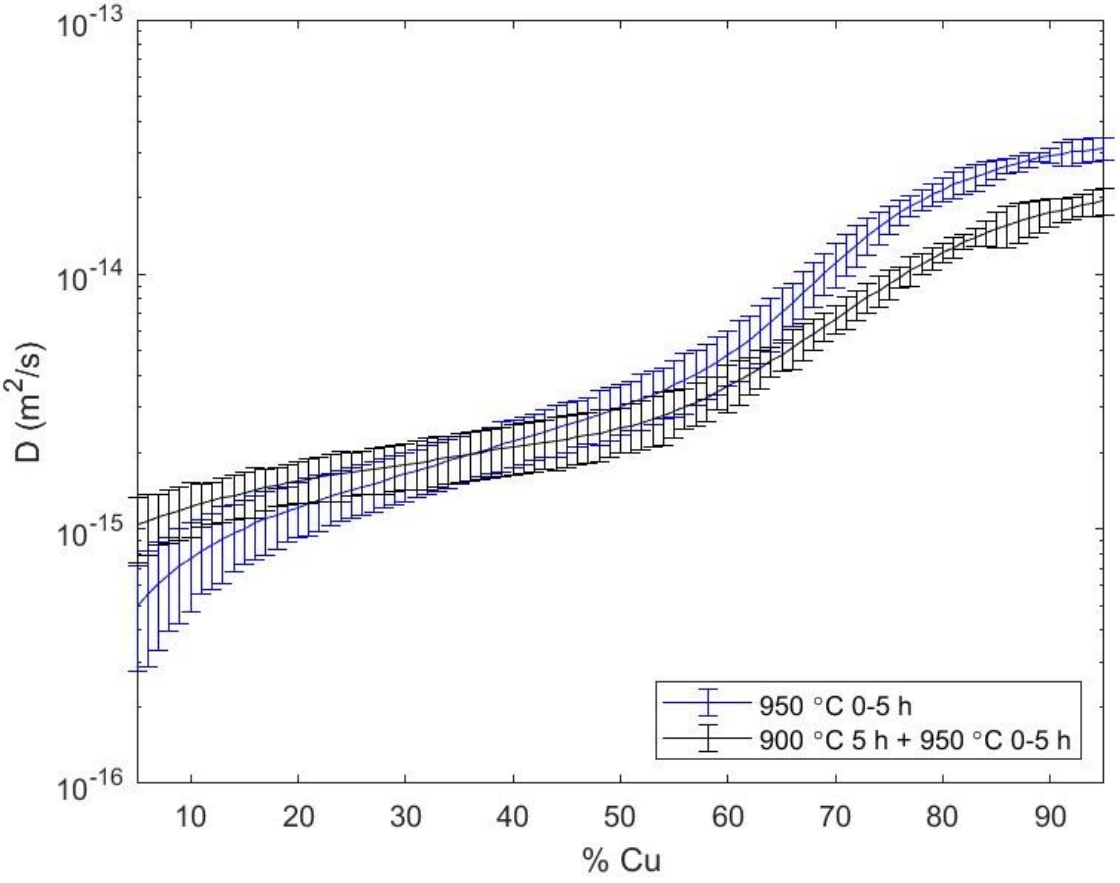

Figure 4.22. Interdiffusion coefficients of Cu-Ni systems with and without initial non-uniform distribution of solute (Type I) at 950°C for 0-5 hours

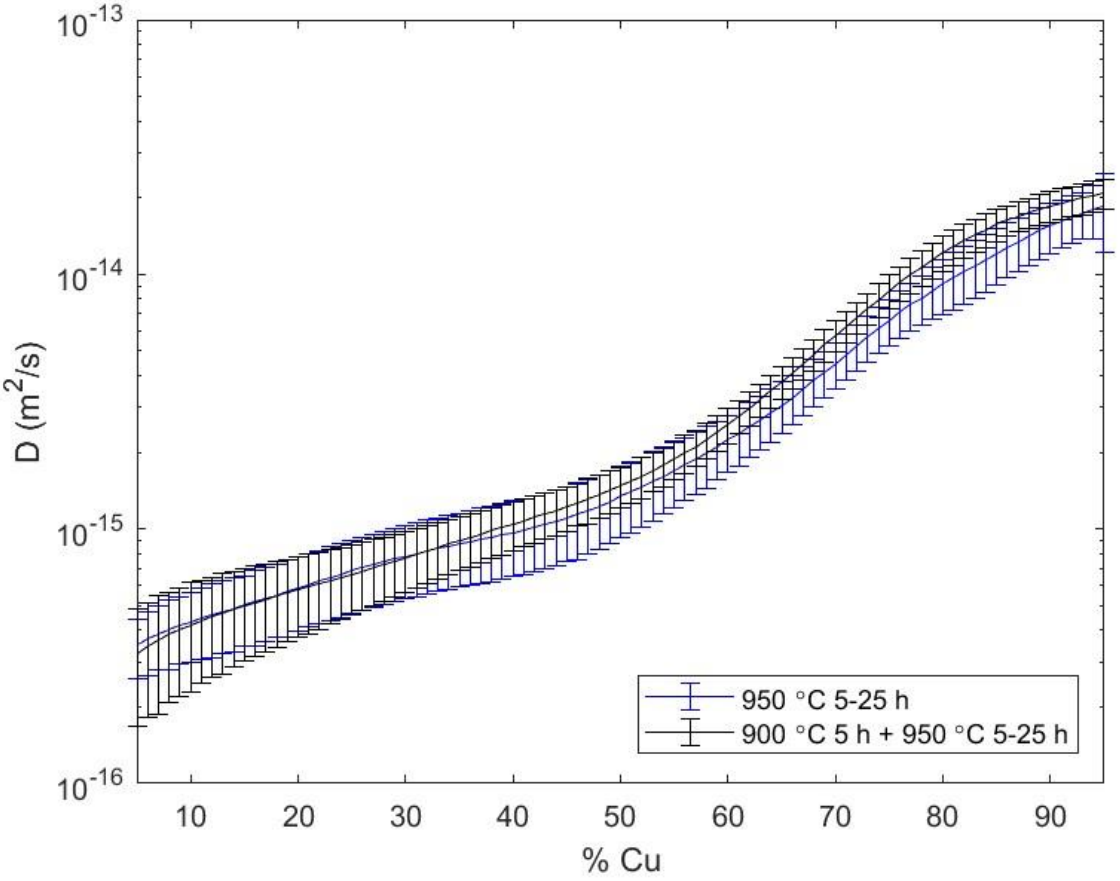

Figure 4.23. Interdiffusion coefficients of Cu-Ni systems with and without initial non-uniform distribution of solute (Type I) at 950°C for 5-25 hours

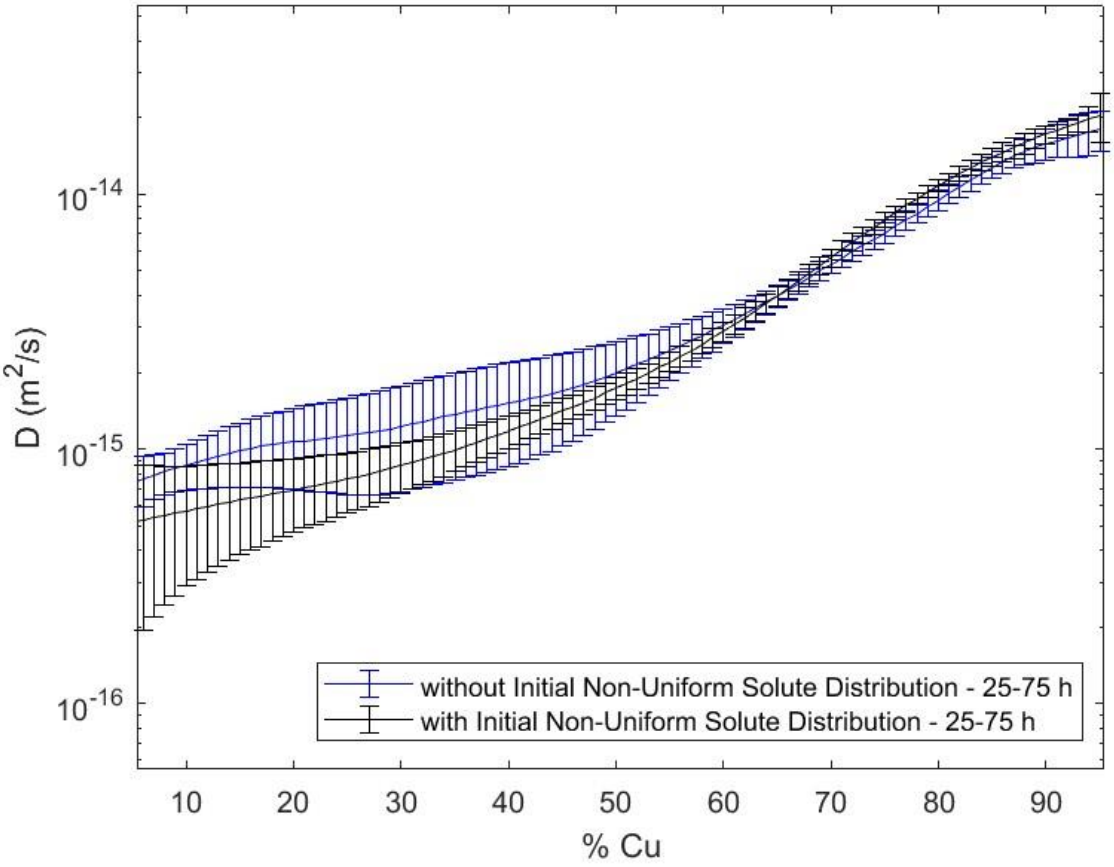

Figure 4.24. Interdiffusion coefficients of Cu-Ni systems with and without initial non-uniform distribution of solute (Type I) at 950°C for 25-75 hours

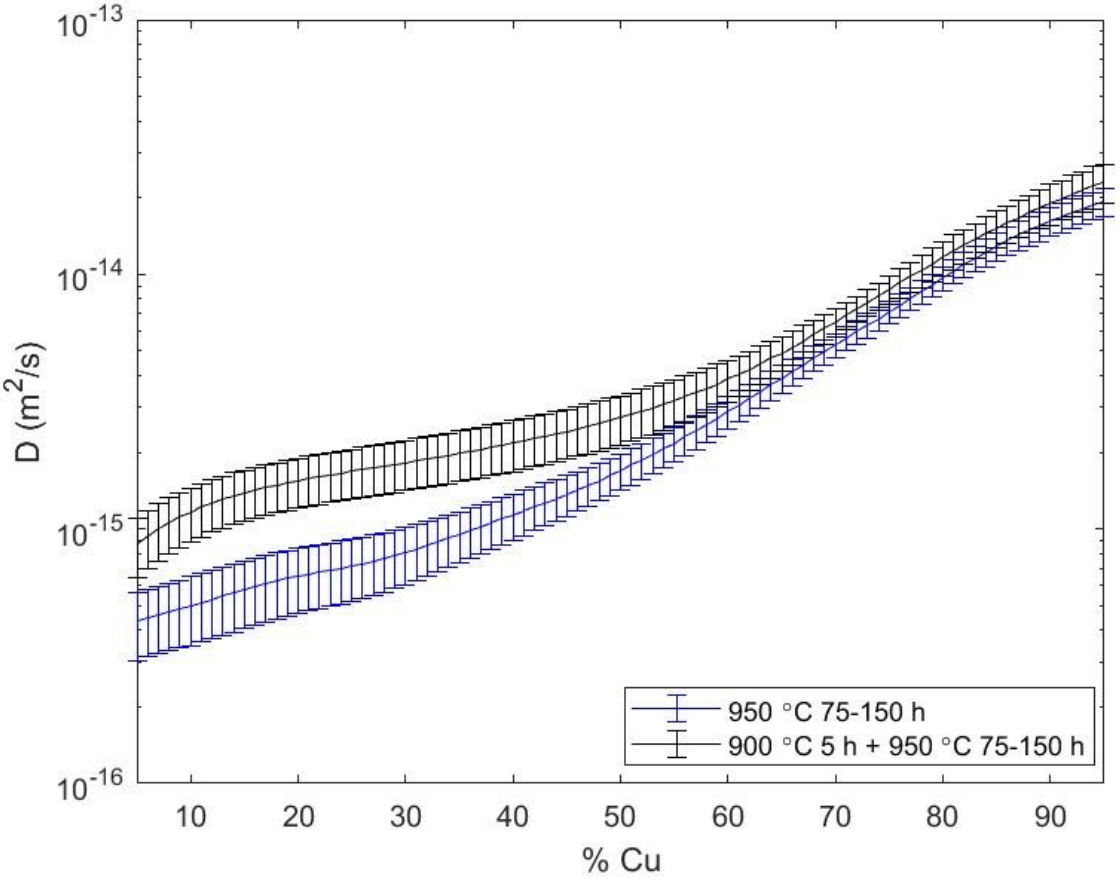

Figure 4.25. Interdiffusion coefficients of Cu-Ni systems with and without initial non-uniform distribution of solute (Type I) at 950°C for 75-150 hours

Table 4.13. p-values of Cu-Ni systems with and without initial non-uniform distribution of solute (Type I) at 950°C

Cu at. %	**5.0**	**10.0**	**15.0**	**20.0**	**25.0**
0-5 h	0.002	< 0.001	0.001	0.001	0.006
5-25 h	0.127	0.007	< 0.001	< 0.001	< 0.001
25-75 h	0.013	0.009	< 0.001	< 0.001	< 0.001
75-150 h	< 0.001	< 0.001	< 0.001	< 0.001	< 0.001
Cu at. %	**30.0**	**35.0**	**40.0**	**45.0**	**50.0**
0-5 h	0.017	0.051	0.216	0.347	0.665
5-25 h	< 0.001	< 0.001	< 0.001	< 0.001	< 0.001
25-75 h	< 0.001	< 0.001	< 0.001	< 0.001	< 0.001
75-150 h	< 0.001	< 0.001	< 0.001	< 0.001	< 0.001
Cu at. %	**55.0**	**60.0**	**65.0**	**70.0**	**75.0**
0-5 h	0.777	0.673	0.019	< 0.001	< 0.001
5-25 h	< 0.001	< 0.001	< 0.001	0.059	0.052
25-75 h	< 0.001	0.083	0.441	0.110	0.782
75-150 h	< 0.001	< 0.001	0.011	0.029	0.019
Cu at. %	**80.0**	**85.0**	**90.0**	**95.0**	
0-5 h	< 0.001	0.005	< 0.001	0.003	
5-25 h	0.003	< 0.001	0.007	0.025	
25-75 h	0.015	0.011	0.090	< 0.001	
75-150 h	0.994	0.759	0.885	0.005	

Table 4.14 Average diffusivity of Cu-Ni systems with and without initial non-uniform distribution of solute (Type I) at 950°C.

Time (hours)	$\boldsymbol{D_{ave}}$ (m^2/s) with Initial non-uniform distribution of solute (Type I)	$\boldsymbol{D_{ave}}$ (m^2/s) No initial non-uniform distribution of solute	Percentage difference	*p*-value
0-5 h	5.483E-15	7.089E-15	29%	< 0.001
5-25 h	4.830E-15	3.97E-15	21%	0.007
25-75 h	4.632E-15	4.725E-15	2%	0.089
75-150 h	5.576E-15	4.345E-15	28%	< 0.001

4.4.2 Influence of Initial Non-uniform Distribution of Solute - Type II

The experimental concentration profiles of the Cu-Ni system with an initial non-uniform distribution of solute - Type II and the Cu-Ni system annealed in a single-stage at 950°C are given in Figure 4.26. As seen for the systems with Type I distribution, the concentration gradient difference decreases as the annealing time increases, while the profiles are very similar for 75 and 150 hours, but an obvious difference is seen for 0 hour and 25 hours. The concentration profiles are presented for (a) 0 hour, (b) 25 hours, (c) 75 hours and (d) 150 hours. The interdiffusion coefficient curves of Type II systems for all time intervals at 950°C are presented in Figures 4.27 to 4.30. Observing the $\widetilde{D}(C)$ curves, there is significant overlap of the error bars for all time intervals, except for 0-5 hours. In comparing the annealing time of 0-5 hours, the curves start to differ at around 40 at. % of Cu.

The p-values of the interdiffusion coefficient throughout the concentration is given in Table 4.15, which show that the values are more significant on the Ni-rich side. Table 4.16 presents the D_{ave} comparison and shows the most significant percentage difference for the shortest annealing times, especially for 0-5 hours in which the difference is 92%.

In general, the interdiffusion coefficient also changes with the presence of an initial non-uniform distribution of solute for Type II systems. This change is more pronounced for 0-5 hours.

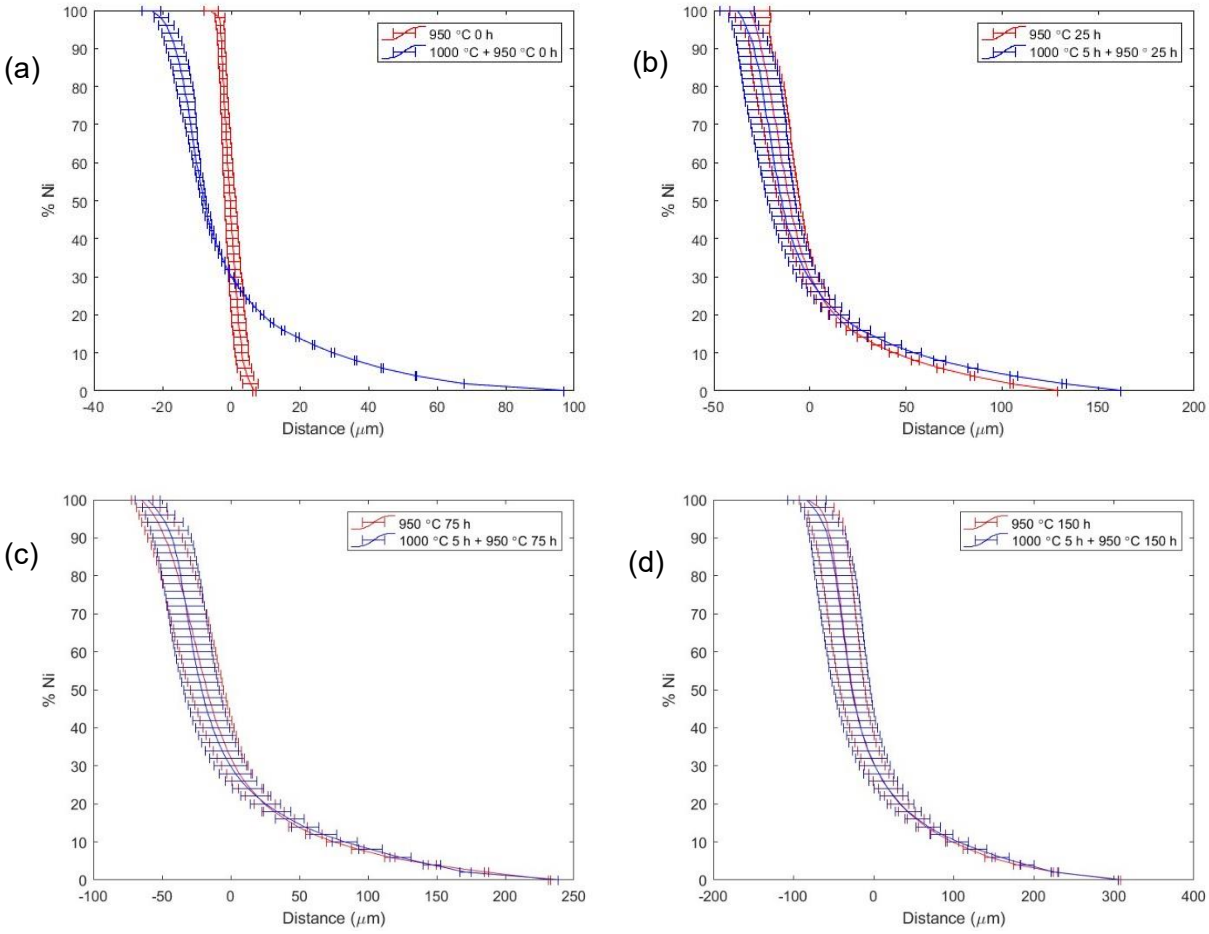

Figure 4.26. Experimental average concentration profiles for single-stage and multi-stage (Type II) treatments at 950°C for (a) 0 hour, (b) 25 hours, (c) 75 hours and (d) 150 hours

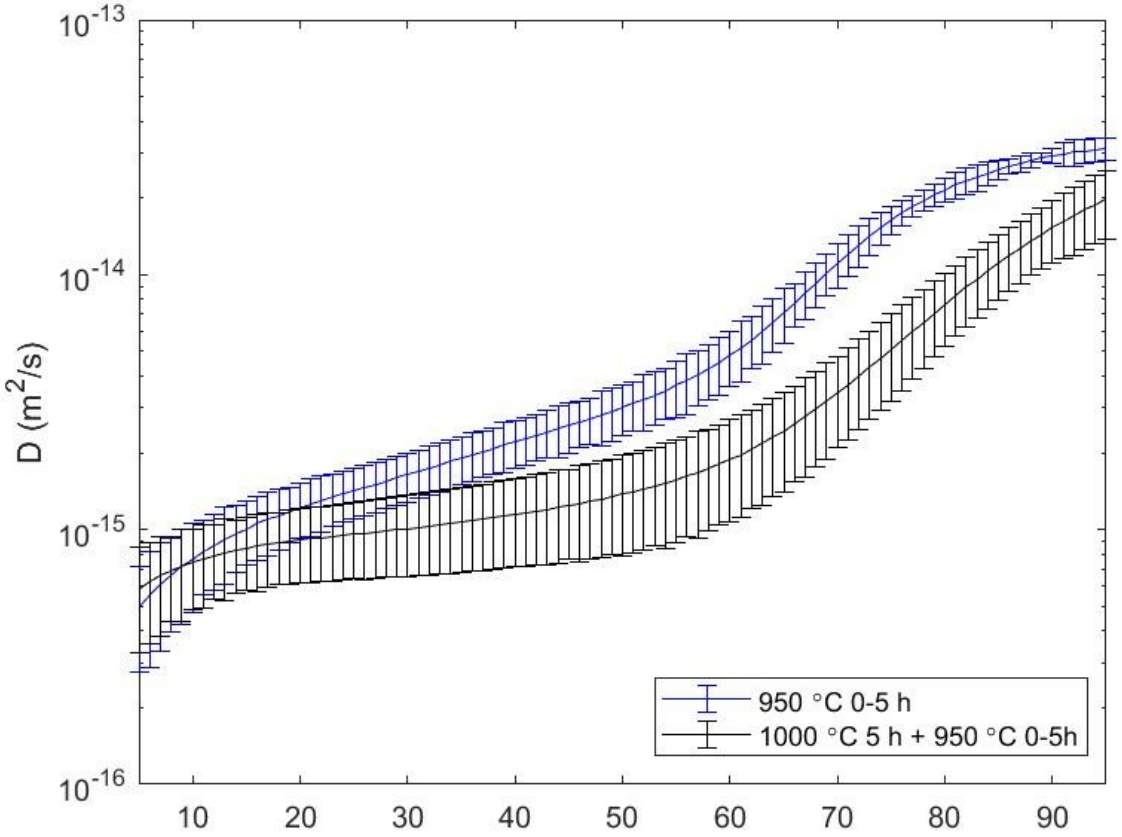

Figure 4.27. Interdiffusion coefficients of Cu-Ni systems with and without initial non-uniform distribution of solute (Type II) at 950°C for 0-5 hours

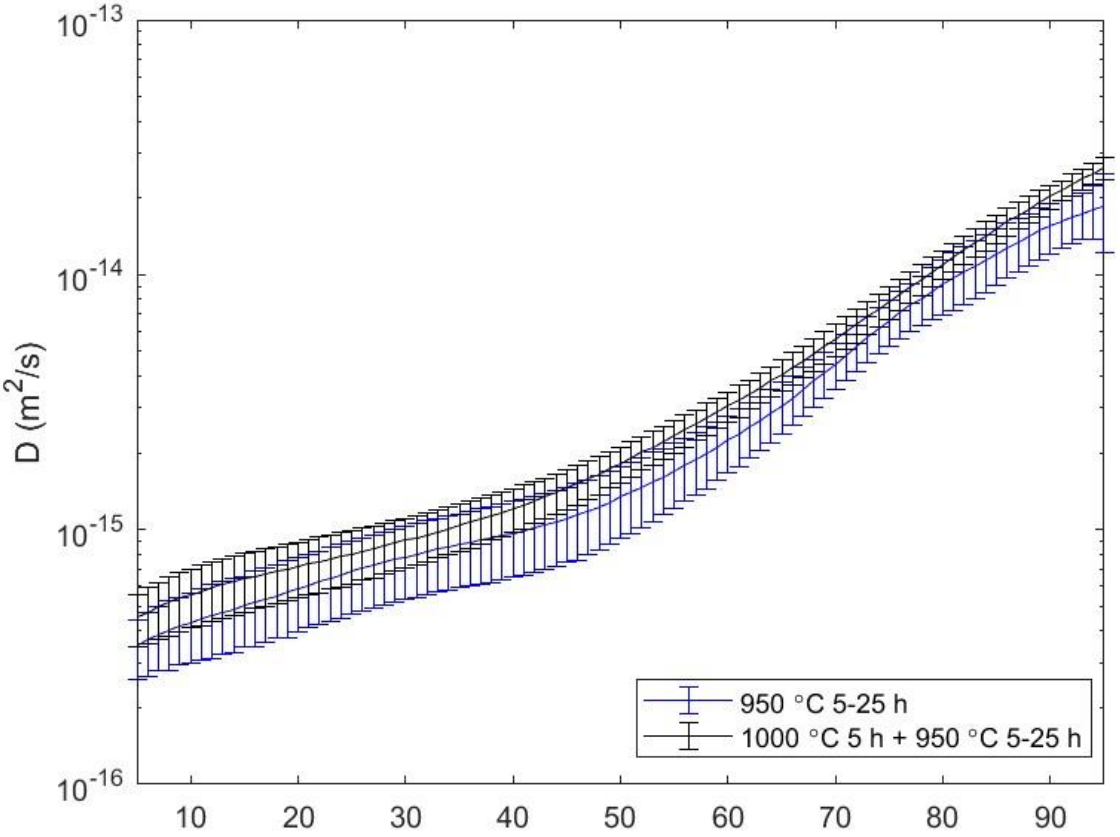

Figure 4.28. Interdiffusion coefficients of Cu-Ni systems with and without initial non-uniform distribution of solute (Type II) at 950°C for 5-25 hours

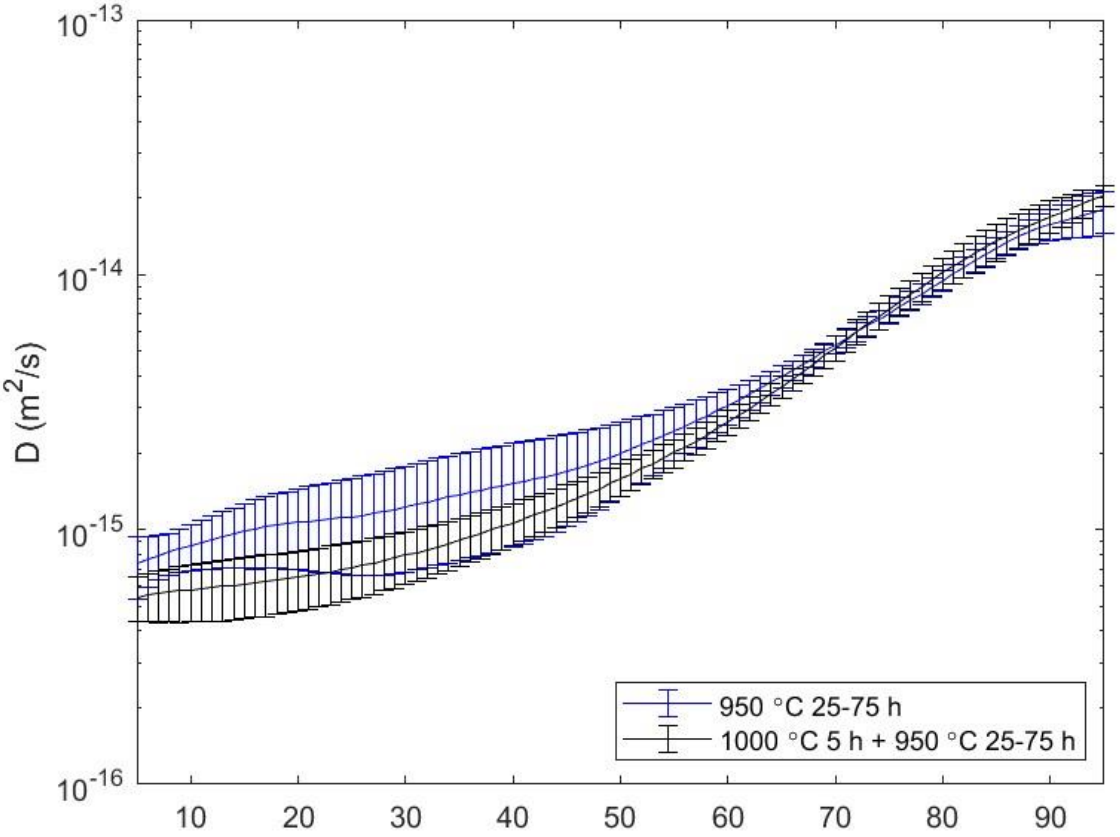

Figure 4.29. Interdiffusion coefficients of Cu-Ni systems with and without initial non-uniform distribution of solute (Type II) at 950°C for 25-75 hours

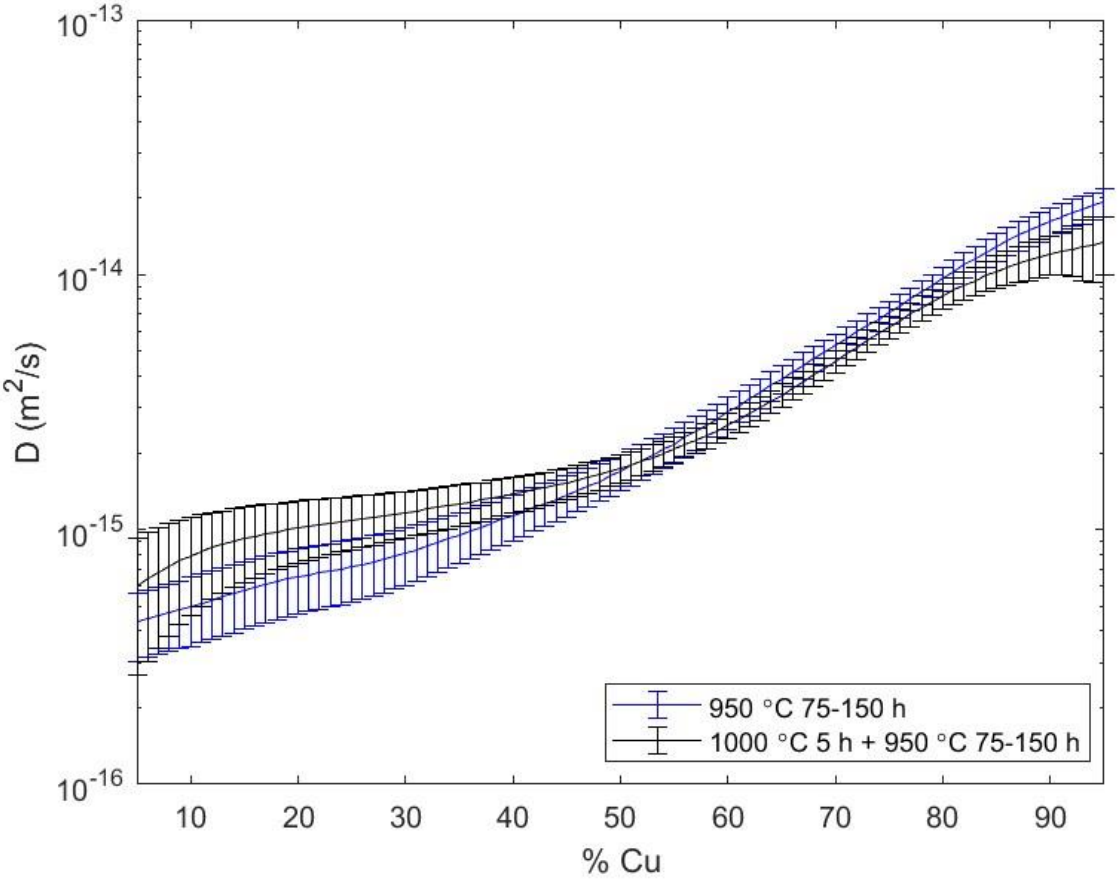

Figure 4.30. Interdiffusion coefficients of Cu-Ni systems with and without initial non-uniform distribution of solute (Type II) at 950°C for 75-150 hours

Table 4.15. *p*-values of Cu-Ni Systems with and without initial non-uniform distribution of solute (Type II) at 950°C

Cu at. %	**5.0**	**10.0**	**15.0**	**20.0**	**25.0**
0-5 h	0.078	0.967	0.596	0.526	0.292
5-25 h	0.374	0.090	< 0.001	< 0.001	< 0.001
25-75 h	< 0.001	0.002	0.137	0.548	0.838
75-150 h	0.083	0.006	< 0.001	< 0.001	< 0.001
Cu at. %	**30.0**	**35.0**	**40.0**	**45.0**	**50.0**
0-5 h	0.0815	0.0672	0.022	< 0.001	< 0.001
5-25 h	< 0.001	< 0.001	< 0.001	< 0.001	< 0.001
25-75 h	0.942	0.922	0.479	0.289	0.717
75-150 h	< 0.001	< 0.001	< 0.001	0.011	0.326
Cu at. %	**55.0**	**60.0**	**65.0**	**70.0**	**75.0**
0-5 h	< 0.001	< 0.001	< 0.001	< 0.001	< 0.001
5-25 h	< 0.001	< 0.001	< 0.001	0.002	0.002
25-75 h	0.225	0.010	< 0.001	0.002	0.291
75-150 h	0.241	0.001	< 0.001	< 0.001	< 0.001
Cu at. %	**80.0**	**85.0**	**90.0**	**95.0**	
0-5 h	< 0.001	< 0.001	< 0.001	0.100	
5-25 h	< 0.001	< 0.001	< 0.001	< 0.001	
25-75 h	0.165	0.064	0.001	< 0.001	
75-150 h	< 0.001	< 0.001	< 0.001	0.018	

Table 4.16. Average diffusivity of Cu-Ni Systems with and without initial non-uniform distribution of solute (Type II) at 950°C

Time (hours)	$\boldsymbol{D_{ave}}$ (m^2/s) with Initial non-uniform distribution of solute (Type I)	$\boldsymbol{D_{ave}}$ (m^2/s) No initial non-uniform distribution of solute	Percentage difference	*p*-value
0-5 h	3.697E-15	7.089E-15	92%	< 0.001
5-25 h	5.079E-15	3.97E-15	22%	< 0.001
25-75 h	4.514E-15	4.725E-15	5%	0.287
75-150 h	3.698E-15	4.345E-15	18%	0.032

4.4.3 Summary of Experimental Verification of Influence of Pre-existing Non-Uniform Solute Distribution

The concentration-dependent interdiffusion coefficient changes with an initial non-uniform distribution of solute in the Cu-Ni system for all temperatures. The underlying cause of these variations are the evolving concentration gradients prompted by the DIS. The changes are more pronounced for Type II, for which the temperature of the first annealing stage is higher (1000°C), towards the Cu-rich side of the concentration range and the shortest annealing time.

The average diffusivity difference between the two systems peaks at 92 % for Type II after 0-5 hours. The interdiffusion coefficient is larger for both Types I and II without an initial non-uniform distribution of solute after 0-5 hours. In general, the interdiffusion coefficient decreases as the annealing time is increased. The only exception is the increase from 25-75 hours to 75-150 hours for Type I. Overall, the time effect discussed in this study shows a distinct trend and is more pronounced in the regions with higher Cu concentration and with shorter annealing times.

5 CONCLUSION

The purpose of this study is to investigate the time effect of the interdiffusion coefficients for the Cu-Ni system under isothermal conditions at temperatures of 900°C, 950°C, and 1000°C. The focus is to determine if DIS is the underlying cause behind the time-dependent changes in the interdiffusion coefficients. By analyzing how the variations in the concentration gradients affect the interdiffusion coefficients throughout the changes in the diffusion process with time, a direct correlation between these two factors can be established.

In order to effectively attribute the changes in the interdiffusion coefficients to the presence of DIS, this study analyzes how changes in the concentration gradients will lead to variation in the interdiffusion coefficients with a constant time and temperature. For the analysis, diffusion couples without an initial solute distribution are compared to those with an initial uniform and non-uniform distribution of solute for the same conditions. These comparative analyses show that the presence or absence of an initial solute distribution has a substantial impact on the concentration gradient, which in turn has a direct impact on the time-dependent changes of the interdiffusion coefficients, that are predominantly driven by the presence of DIS.

Several conclusions can be drawn from this work:

1. Across all of the temperatures investigated, the concentration-dependent interdiffusion coefficients of the Cu-Ni system isothermally varied with time.
2. The concentration-dependent interdiffusion of the Cu-Ni system varies based on the presence of an initial solute distribution, for both uniform and non-uniform distributions.
3. The changes in the interdiffusion coefficient for the same time and temperatures, caused by the presence of an initial solute distribution, are driven by the difference in the

concentration gradient. This is a strong indicator that the DIS is the cause of this phenomenon.

4. The changes in the interdiffusion coefficients are more pronounced during the initial phases of the diffusion process, which means that as the diffusion time increases, the variation of $\widetilde{D}(C)$ decreases. The changes are also more evident in the Cu-rich regions of the concentration range.
5. These observations provide insights into the role of DIS in the time-dependent behavior of interdiffusion in a Cu-Ni system.

6 LIMITATIONS AND FUTURE WORK RECOMMENDATIONS

Despite the insights from this study, there are still some limitations of this work, as follows:

1. The two-profile analytical method used to calculate the interdiffusion coefficients does not provide accurate results for the extreme ends of the concentration range. For example, the results are only reliable for the concentration range of 5-95 % for the pure Cu-Ni system.
2. The time effect has not been explored for impurity diffusion coefficients.
3. It is assumed that the molar volume of the Cu-Ni system does not considerably change throughout the diffusion process.

Based on the limitations, some recommendations for future works are as follows:

1. The changes in interdiffusion coefficients with time for other couple configurations can consider factors such as:
    a. Different geometries,
    b. Other binary systems, including those that form intermediate phases between the ultimate compositions, and
    c. Multi-component systems.
2. Other methods to calculate the interdiffusion and impurity coefficients can be taken into consideration, such as a forward simulation analysis or other numerical methods.

REFERENCES

[1] Mehrer, H. (2007). *Diffusion in solid materials: fundamentals, methods, materials, diffusion-controlled processes* (Vol. 155). Springer.

[2] Balluffi, R., Allen, S. M., Carter, W. C., & Kemper, R. A. (2005). *Kinetics of materials*. J. Wiley & Sons.

[3] Zhong, Chen, L., & Zhang, L. (2020). High-throughput determination of high-quality interdiffusion coefficients in metallic solids: a review. *Journal of Materials Science*, *55*(24), 10303–10338. https://doi.org/10.1007/s10853-020-04805-1

[4] Campbell, D.R., Tu, K. N., & Robinson, R. E. (1976). Interdiffusion in a bulk couple of lead and lead-50 wt.% indium alloy. *Acta Metallurgica*, *24*(7), 609–614. https://doi.org/10.1016/0001-6160(76)90080-8

[5] Kucera, J., Ciha, K., & Stransky, K. (1977). Interdiffusion in the Co-Ni system-I concentration penetration curves and interdiffusion coefficients. *Czechoslovak Journal of Physics, 27*(7), 758–768. https://doi.org/10.1007/BF01589317

[6] Haebicek, J., Kucera, J., & Stransky, K. (1975). Determination of interdiffusion coefficients in the Co-Ni system with the use of spline functions. *Czechoslovak Journal of Physics, 25*(10), 1181–1191. https://doi.org/10.1007/BF01798699

[7] Kirkendall, E., Thomassen, L., & Upthegrove, C. (1938). *Rates of diffusion of copper and zinc in alpha brass.*

[8] Olaye, O., & Ojo, O. A. (2021). Time variation of concentration-dependent interdiffusion coefficient obtained by numerical simulation analysis. *Materialia*, *16*, 101056–. https://doi.org/10.1016/j.mtla.2021.101056

[9] Neubauer, C.M., Mari, D., & Dunand, D. C. (1994). Diffusion in the nickel-rhenium system. *Scripta Metallurgica et Materialia*, *31*(1), 99–104. https://doi.org/10.1016/0956-716X(94)90102-3

[10] Resnick, R., & Baluffi, R.W. (1955). Diffusion of Zinc and Copper in Alpha and Beta Brasses. *JOM 7*, 1004-1010. https://doi.org/10.1007/BF03377601

[11] Mehl. R. F., & Rhines, F. N. (1938). Rates of diffusion in the alpha solid solutions of copper. AIME TRANS, 128, 185–221. == [49]

[12] Jain, R.K., & van Overstraeten, R. J. (1974). Calculation of the diffusion induced stresses in silicon. *Physica Status Solidi. A, Applied Research*, *25*(1), 125–130. https://doi.org/10.1002/pssa.2210250109

[13] Stephenson, G.B. (1988). Deformation during interdiffusion. *Acta Metallurgica*, *36*(10), 2663–2683. https://doi.org/10.1016/0001-6160(88)90114-9

[14] Larcht'e, F.C., & Cahn, J. l. (1982). The effect of self-stress on diffusion in solids. *Acta Metallurgica*, *30*(10), 1835–1845. https://doi.org/10.1016/0001-6160(82)90023-2

[15] Daruka, I., Szabó, I. A., Beke, D. L., Cserháti, C., Kodentsov, A., & Van Loo, F. J. J. (1996). Diffusion-induced bending of thin sheet couples: Theory and experiments in Ti-Zr system. *Acta Materialia*, *44*(12), 4981–4993. https://doi.org/10.1016/S1359-6454(96)00099-7

[16] Chu, J.L., & Lee, S. (1994). The effect of chemical stresses on diffusion. *Journal of Applied Physics*, *75*(6), 2823–2829. https://doi.org/10.1063/1.356174

[17] Zhang, X., Hao, F., Chen, H., & Fang, D. (2015). Diffusion-induced stress and delamination of layered electrode plates with composition-gradient. *Mechanics of Materials*, *91*, 351–362. https://doi.org/10.1016/j.mechmat.2015.04.016

[18] Beke, D. L., Erdélyi, Z., & Parditka, B. (2011). Effect of Diffusion Induced Driving Forces on Interdiffusion - Stress Development/Relaxation and Kinetics of Diffusion Processes. In Defect and Diffusion Forum (Vols. 309–310, pp. 113–120). Trans Tech Publications, Ltd. https://doi.org/10.4028/www.scientific.net/ddf.309-310.113

[19] Beke, D.L., Szabó, I. A., Erdélyi, Z., & Opposits, G. (2004). Diffusion-induced stresses and their relaxation. *Materials Science & Engineering. A, Structural Materials: Properties, Microstructure and Processing*, *387*, 4–10. https://doi.org/10.1016/j.msea.2004.01.065

[20] Yang, F. (2021). Generalized Theory for Diffusion-Induced Stress. *Journal of the Electrochemical Society*, *168*(4), 40520–. https://doi.org/10.1149/1945-7111/abf411

[21] Beke, D.L., Erdélyi, Z., Szabó, I. A., Beke, D. L. (Dezső L., & Erdélyi, Z. (Zoltán). (2007)." Stress Evolution in Thin Films; Diffusion and Reactions" *Diffusion and stresses: proceedings of the International Workshop on Diffusion and Stresses, Lillafüred, Hungary, September 19-22, 2006*. Trans Tech Publications Ltd.

[22] Paul, A., Laurila, T., Vuorinen, V., & Divinski, S. V. (2014). *Thermodynamics, Diffusion and the Kirkendall Effect in Solids* (1st ed. 2014.). Springer International Publishing. https://doi.org/10.1007/978-3-319-07461-0

[23] Shewmon, P. (1991). *Diffusion in Solids*. Springer International Publishing AG.

[24] Tang, Y., & Zhang, L. (2018). Effect of Thermal Vacancy on Thermodynamic Behaviors in BCC W Close to Melting Point: A Thermodynamic Study. *Materials*, *11*(9), 1648–. https://doi.org/10.3390/ma11091648

[25] Murch, G.E. (2001). Ferrite and Austenite: Diffusion, Bulk and Interfacial, Encyclopedia of Materials: Science and Technology. Elsevier.3009-3012 ,https://doi.org/10.1016/B0-08-043152-6/00536-2.

[26] Herzig, C. & Mishin, Y. (2006). Grain Boundary Diffusion in Metals. In *Diffusion in Condensed Matter* (pp. 337–366). Springer Berlin Heidelberg. https://doi.org/10.1007/3-540-30970-5_8

[27] Wang, Z., Fang, L., Cotton, I., & Freer, R. (2015). Ni–Cu interdiffusion and its implication for ageing in Ni-coated Cu conductors. *Materials Science & Engineering. B, Solid-State Materials for Advanced Technology*, *198*, 86–94. https://doi.org/10.1016/j.mseb.2015.04.006

[28] Radomir, I., Geamăn, V., & Stoicănescu, M. (2012). Densification Mechanisms Made During Creep Techniques Applied to the Hot Isostatic Pressing. *Procedia, Social and Behavioral Sciences*, *62*, 779–782. https://doi.org/10.1016/j.sbspro.2012.09.131

[29] Gusak, A.M., Shirinyan, A., Zaporozhets, T., Lyashenko, Y. O., Kornienko, S. , & Pasichnyy , M. O. (2011). *Diffusion-controlled solid-state reactions: in alloys, thin films, and nano systems*. Wiley-VCH. https://doi.org/10.1002/9783527631025

[30] Baheti, V.A., Ravi, R., & Paul, A. (2013). Interdiffusion study in the Pd–Pt system. *Journal of Materials Science. Materials in Electronics*, *24*(8), 2833–2838.

[31] Kavakbasi, B.T., Golovin, I. S., Paul, A., & Divinski, S. V. (2017). *On the analysis of composition profiles in binary diffusion couples: systems with a strong compositional dependence of the interdiffusion coefficient*. https://doi.org/10.48550/arxiv.1707.07324

[32] Eastman, C.M., Zhang, Q., & Zhao, J.-C. (2020). Diffusion Coefficients and Phase Equilibria of the Cu-Zn Binary System Studied Using Diffusion Couples. *Journal of Phase Equilibria and Diffusion*, *41*(5), 642–653. https://doi.org/10.1007/s11669-020-00831-3

[33] Karunaratne, M.S.A, Carter, P., & Reed, R. (2000). Interdiffusion in the face-centred cubic phase of the Ni–Re, Ni–Ta and Ni–W systems between 900 and 1300°C. *Materials Science &*

Engineering. A, Structural Materials : Properties, Microstructure and Processing, *281*(1), 229–233. https://doi.org/10.1016/S0921-5093(99)00705-4 == [34]

[34] Santra, S., Dong, H., Laurila, T., & Paul, A. (2014). Role of different factors affecting interdiffusion in Cu(Ga) and Cu(Si) solid solutions. *Proceedings of the Royal Society. A, Mathematical, Physical, and Engineering Sciences*, *470*(2161), 20130464–20130464. https://doi.org/10.1098/rspa.2013.0464

[35] Chen, Z., Liu, Z.-K., & Zhao, J.C. (2018). Experimental Determination of Impurity and Interdiffusion Coefficients in Seven Ti and Zr Binary Systems Using Diffusion Multiples. *Metallurgical and Materials Transactions. A, Physical Metallurgy and Materials Science*, *49*(7), 3108–3116. https://doi.org/10.1007/s11661-018-4645-9

[36] Liu, X.J., Yu, Y., Lu, Y., Luo, Y. S., Han, J. J., & Wang, C. P. (2018). Interdiffusion and Atomic Mobilities in fcc Co-Ga and Co-V Alloys. *Journal of Phase Equilibria and Diffusion*, *39*(1), 2–10. https://doi.org/10.1007/s11669-017-0598-8

[37] Ahmed, T., Belova, I. V., Evteev, A. V., Levchenko, E. V., & Murch, G. E. (2015). Comparison of the Sauer-Freise and Hall Methods for Obtaining Interdiffusion Coefficients in Binary Alloys. *Journal of Phase Equilibria and Diffusion*, *36*(4), 366–374. https://doi.org/10.1007/s11669-015-0392-4

[38] Matano, C. (1933). On the Relation Between the Diffusion-Coefficients and Composition of Solid Metals (The Nickel-Copper System). *Jpn. J. Phys., 8*, 109-113.

[39] Boltzmann, L. (1894). Integration of the Diffusion Equation with Variable Diffusion Coefficients (University of North Texas, Trans.). *Ann. Phys. 53*, 959-964

[40] Schmid, K., & Roth, J. (2002). Concentration dependent diffusion of carbon in tungsten. *Journal of Nuclear Materials*, *302*(2), 96–103. https://doi.org/10.1016/S0022-3115(02)00807-3

[41] Zhao, Y., Pang, T., He, J., Tao, X., Chen, H., Ouyang, Y., & Du, Y. (2018). Interdiffusion behaviors and mechanical properties of Cu-Zr system. *Calphad*, *61*, 92–97. https://doi.org/10.1016/j.calphad.2018.02.008

[42] Sauer, F., & Freise, V. (1962). Diffusion in Binary Mixtures Showing a Volume Change. *Z. Elektrochem, 66*, 353-362.

[43] Zhao, J.C. Phase diagram determination using diffusion multiples. In *Methods for Phase Diagram Determination*; Zhao, J.C., Ed.; Elsevier: New York, NY, USA, 2007; pp. 246–272

[44] Campbell. (2005). A New Technique for Evaluating Diffusion Mobility Parameters. *Journal of Phase Equilibria and Diffusion*, *26*(5), 435–440. https://doi.org/10.1361/154770305X66484

[45] Olaye, O., & Ojo, O. A. (2021). A New Analytical Method for Computing Concentration-Dependent Interdiffusion Coefficient in Binary Systems with Pre-existing Solute Concentration Gradient. *Journal of Phase Equilibria and Diffusion*, *42*(2), 303–314. https://doi.org/10.1007/s11669-021-00883-z

[46] Takei, W.J., & Francombe, M. H. (1968). Measurement of diffusion-induced strains at metal bond interfaces. *Solid-State Electronics*, *11*(2), 205–208. https://doi.org/10.1016/0038-1101(68)90080-4

[47] Opposits, G., Szabó, S., Beke, D. L., Guba, Z., & Szabó, I. A. (1998). Diffusion-induced bending of Cu-Ni thin sheet diffusion couples. *Scripta Materialia*, *39*(7), 977–983. https://doi.org/10.1016/S1359-6462(98)00228-0

[48] Marenych, O., & Kostryzhev, A. (2020). Strengthening Mechanisms in Nickel-Copper Alloys: A Review. *Metals (Basel)*, *10*(10), 1358–. https://doi.org/10.3390/met10101358

[49] Ijima, Y., Hirano, K-C., Kikuchi, M. (1982). Determination of Intrinsic Diffusion Coefficients in a Wide Concentration Range of a Cu-Ni Couple by the Multiple Markers Method. Transactions of the Japan Institute of Metals, 23(1), 19-23.

[50] Wang, J., Liu, H. S., Liu, L. B., & Jin, Z. P. (2008). Assessment of diffusion mobilities in FCC Cu–Ni alloys. *Calphad*, *32*(1), 94–100. https://doi.org/10.1016/j.calphad.2007.08.001

[51] Prussin, S. (1961). Generation and Distribution of Dislocations by Solute Diffusion. *Journal of Applied Physics*, *32*(10), 1876–1881. https://doi.org/10.1063/1.1728256

[52] Hirsch, J. (2011). 23 - Aluminium sheet fabrication and processing. In *Fundamentals of aluminium metallurgy* (pp. 719–746). Elsevier Ltd. https://doi.org/10.1533/9780857090256.3.719

[53] Imanami, Y., Murakami, M., Nakada, N., Tsuchiyama, T., & Takaki, S. (2009). Contribution of Soft Copper Particle on Work Hardening Behavior in Ferritic Iron. *ISIJ International*, *49*(8), 1225–1228. https://doi.org/10.2355/isijinternational.49.1225

[54] Gottstein, G. (2011). Metal Forming (Cold): Dislocation Mechanisms and Microstructural Changes. In *Encyclopedia of Materials: Science and Technology* (pp. 5394–5401). Elsevier Ltd. https://doi.org/10.1016/B0-08-043152-6/00941-4

[55] Makita, H., Hanada, S., & Izumi, O. (1988). Recrystallization in cold-rolled pure nickel. *Acta Metallurgica*, *36*(2), 403–412. https://doi.org/10.1016/0001-6160(88)90016-8

[56] Annealing and Recrystallization of Coppers, *Heat Treating of Nonferrous Alloys*, Vol 4E, *ASM Handbook*, Edited By George E. Totten, ASM International, 2016, p 325–334, https://doi.org/10.31399/asm.hb.v04e.a0006278

[57] Humphreys, F.J., & Hatherly, M. (2004). *Recrystallization and related annealing phenomena* (2nd ed.). Elsevier.

[58] Benchabane, G., Boumerzoug, Z., Thibon, I., & Gloriant, T. (2008). Recrystallization of pure copper investigated by calorimetry and microhardness. *Materials Characterization*, *59*(10), 1425–1428. https://doi.org/10.1016/j.matchar.2008.01.002

[59] Chen, W., Li, Q., & Zhang, L. (2017). A Novel Approach to Eliminate the Effect of External Stress on Interdiffusivity Measurement. *Materials*, *10*(8), 961–. https://doi.org/10.3390/ma10080961

[60] Saha, S., Johnson, M., Altayaran, F., Wang, Y., Wang, D., & Zhang, Q. (2020). Electrodeposition Fabrication of Chalcogenide Thin Films for Photovoltaic Applications. *Electrochem (Basel, Switzerland)*, *1*(3), 286–321. https://doi.org/10.3390/electrochem1030019

[61] *Piecewise Cubic Hermite Interpolating Polynomial (PCHIP) - MATLAB pchip*. (n.d.). https://www.mathworks.com/help/matlab/ref/pchip.html

[62] Khan, M. S.H. (2011). Standard Deviation. In: Lovric, M. (eds) International Encyclopedia of Statistical Science. Springer, Berlin, Heidelberg. https://doi-org.uml.idm.oclc.org/10.1007/978-3-642-04898-2_535

[63] Lovric. (2011). *International Encyclopedia of Statistical Science* (Lovric, Ed.; 1st ed. 2011.). Springer Berlin Heidelberg. https://doi.org/10.1007/978-3-642-04898-2